Finite-size effects and Coulomb interactions in quantum Monte Carlo calculations for homogeneous systems with periodic boundary conditions

Louisa M. Fraser and W. M. C. Foulkes
Condensed Matter Theory Group, Blackett Laboratory, Imperial College of Science, Technology and Medicine, Prince Consort Road, London SW7 2BZ, United Kingdom

G. Rajagopal, R. J. Needs, S. D. Kenny, and A. J. Williamson
Theory of Condensed Matter Group, Cavendish Laboratory, Madingley Road, Cambridge CB3 0HE, United Kingdom
(Received 1 August 1995)

Quantum Monte Carlo (QMC) calculations are only possible in finite systems and so solids and liquids must be modeled using small simulation cells subject to periodic boundary conditions. The resulting finite-size errors are often corrected using data from local-density functional or Hartree-Fock calculations, but systematic errors remain after these corrections have been applied. The results of our jellium QMC calculations for simulation cells containing more than 600 electrons confirm that the residual errors are significant and decay very slowly as the system size increases. We show that they are sensitive to the form of the model Coulomb interaction used in the simulation cell Hamiltonian and that the usual choice, exemplified by the Ewald summation technique, is not the best. The finite-size errors can be greatly reduced and the speed of the calculations increased by a factor of 20 if a better choice is made. Finite-size effects plague most methods used for extended Coulomb systems and many of the ideas in this paper are quite general: they may be applied to any type of quantum or classical Monte Carlo simulation, to other many-body approaches such as the GW method, and to Hartree-Fock and density-functional calculations.

I. INTRODUCTION

Most local-density functional (LDF) calculations for extended systems use Bloch's theorem and hence rely on translational symmetry. Indeed, the simplifying power of Bloch's theorem is so great that translational symmetry is often imposed even on aperiodic systems: the region of interest — perhaps consisting of a point defect and a few of the surrounding atoms — is periodically repeated to make an artificial crystal so that standard k-space methods can be used. The periodically repeated region is called the supercell and is made as large as is computationally feasible, but there are significant finite-size errors for practical system sizes.

One can easily make plausible arguments predicting how these finite-size errors should depend on the linear dimension L of the supercell. If the supercell is charge neutral but has a nonzero dipole moment, for example, then one might expect that dipole-dipole interactions between supercells would contribute unwanted terms of order L^{-3} to the total energy. In fact, as shown by Makov and Payne,[1] one can do better than this if the supercell Hamiltonian is defined appropriately.

In LDF calculations for perfect crystals the periodicity is not imposed artificially and so there are no finite-size errors in principle. There are still errors in practice, however, because discrete quadratures are used to approximate Brillouin-zone integrals. These k-point sampling errors are often explained using the mathematical theory of quadrature, but a different approach is to view them as finite-size effects. Consider a large but finite crystal containing many unit cells. The application of periodic boundary conditions at the surfaces of this crystal determines the set of allowed k points in the Brillouin zone. As long as the crystal is large, the quadrature grid is fine, and the results are almost the same as for an infinite system; but when the crystal is small, the k-point sampling grid is coarse, and the Brillouin-zone integration errors are large. The sampling errors therefore reflect the differences between the finite crystal implied by the integration grid and the infinite crystal we would like to model. Not all k-point sampling schemes fit into the framework of this argument, of course, but the ones that do happen to be the ones of interest for quantum Monte Carlo (QMC) calculations.[2,3]

We have now mentioned both types of finite-size error present in LDF calculations. The supercell errors described in the first two paragraphs arise when a periodic ''model Hamiltonian'' is used to represent an aperiodic system; the system remains infinite in extent but the periodicity is imposed artificially. The k-point sampling errors are caused by the boundary conditions used to make an infinite periodic system finite, and hence affect calculations for perfect crystals as well as supercell calculations.

This paper is concerned with finite-size errors in QMC calculations for infinite periodic systems; errors in QMC calculations for aperiodic systems will not be considered. Since QMC methods can only be applied when the number of particles is finite, infinite periodic systems must be modeled using finite simulation cells subject to periodic boundary conditions. The replacement of an infinite system by a finite one introduces errors analogous to the k-point sampling errors in a LDF calculation. The current practical limit on the size of the simulation cell is a few hundred electrons, corresponding to perhaps a few tens of k points in the primitive Brillouin zone, and so it is not surprising that these finite-size errors are large. Furthermore, although the cost of a LDF calculation rises only linearly with the number of k points,

the cost of a QMC calculation rises more rapidly and so it is harder to decrease the QMC finite-size error by increasing the system size.

Finite-size errors in QMC calculations for infinite periodic systems are not well understood. They decay rather slowly as functions of L, so the obvious tactic of increasing the size of the simulation cell until they go away is impractical. The usual approach is to assume that they are the same as the finite-size errors in LDF or Hartree-Fock (HF) calculations for the same simulation cell (i.e., with the appropriate restricted k-point sampling) and to correct them using LDF or HF results.[4,5] Systematic errors remain after these corrections have been applied, however, and our large homogeneous electron gas (HEG) calculations have confirmed that these residual finite-size effects are significant (typically 0.1 or 0.2 eV per electron) and very slowly decaying. Past attempts to reduce the residual errors have used Coulomb and correlation corrections of various types,[6–8] but it has not been possible to make a reliable extrapolation to the infinite system size limit without carrying out simulations for several different system sizes.

The existence of the long-ranged residual errors shows that the finite-size effects in QMC calculations differ qualitatively from the k-point sampling errors in LDF calculations. The finite simulation cell used to model the infinite system is the same in both cases, and so the differences must reflect the different ways in which the two methods treat the electron-electron interaction. In LDF calculations, the interaction is replaced by an effective one-electron potential, which depends only on the charge density and is the same in every unit cell of the crystal. In QMC calculations, however, it is necessary to evaluate the full interacting Coulomb energy, which depends on the current positions of all the (pointlike) electrons in every unit cell of the crystal. The electronic positions differ from cell to cell and hence it is impossible to avoid approximating the Coulomb energy when the large crystal is replaced by a small simulation cell subject to periodic boundary conditions. This approximation introduces an extra finite-size error that is not present in LDF calculations and is the main cause of the long-ranged residual errors.

In most calculations the full Coulomb energy is replaced by the Ewald energy,[9] which is a periodic function of the positions of the N electrons in the simulation cell (these are the only electrons in the simulation). The periodicity implies that the Ewald energy does not change when any single electron is translated by a simulation cell lattice vector, but such a translation does change the Coulomb energy of the infinite system. This is reminiscent of the LDF supercell method, in which a periodic model Hamiltonian is used to approximate an aperiodic system; the main difference is that now we must use a model Hamiltonian even for perfect crystals.

There is, of course, no need to use periodic boundary conditions: the small group of atoms in a QMC calculation for a solid or liquid could be treated as a cluster embedded in a vacuum or a dielectric. In practice, however, the number of atoms is so small that almost all would then be on or near a surface and the cluster properties would not resemble those of the solid or liquid. The use of periodic boundary conditions avoids this problem by wrapping the finite system around into a torus with no surfaces, but the price is that the long-ranged Coulomb interactions must now be replaced by the model Ewald interactions.

The main result of our work has been to show that the long-ranged residual errors are Coulomb finite-size effects associated with the use of the Ewald model Hamiltonian (we have already explained that these Coulomb errors are not present in LDF calculations and hence are not removed when LDF finite-size corrections are applied). Having identified the cause of the long-ranged errors, we have also been able to see how to alter the form of the model simulation cell Hamiltonian to reduce them. The freedom to choose the model Hamiltonian to minimize the finite-size errors has not been exploited in previous QMC work (although it has in classical simulations[10–13]), but the long-ranged Coulomb errors disappear if the right choice is made.

Perhaps surprisingly, the smallest finite-size errors are obtained when the complicated Ewald interactions in the simulation cell Hamiltonian are replaced by truncated Coulomb interactions. If this simplification is combined with the use of short-ranged Jastrow factors of the type introduced by Ortiz and Ballone,[14,15] a typical HEG QMC calculation is sped up by a factor of at least 20 and the finite-size errors are much reduced. The remaining errors are negligible even for quite small system sizes, and the extrapolation to the infinite system size limit is unnecessary in many cases.

For simplicity, this paper concentrates on the homogeneous electron gas. It is clear that the ideas also apply to other homogeneous systems such as electron-hole liquids and electron gases containing positrons, but the generalization to inhomogeneous systems such as solids is more difficult and will be dealt with in a future paper.

The rest of the paper is organized as follows. In Sec. II we describe the variational QMC method, taking particular care to explain the model Coulomb interactions used in the simulation cell Hamiltonian. In Sec. III we discuss the usual finite-size corrections applied to QMC results, and present some HEG calculations that demonstrate the presence of the long-ranged residual finite-size effects referred to above. We point out that the existence of such long-ranged effects is unexpected given the short range of the exchange-correlation hole, and argue that the problem must be due to the form of the simulation cell Hamiltonian. In Sec. IV we summarize the problems associated with defining Coulomb potentials in periodic solids, and give physically motivated derivations of the fundamental results of the classic (but mathematically complicated) paper by de Leeuw, Perram, and Smith.[16] In Sec. V we show how the general theory of Sec. IV applies to the special case of QMC calculations, and explain how the conventional (Ewald) choice of boundary conditions for the solution of Poisson's equation inevitably produces large finite-size errors. Two different solutions to this problem are presented in Sec. VI, backed up by the results of an extensive series of HEG QMC calculations. Section VII recaps what we have learned about finite-size effects in the HEG, and emphasizes again that the work described in this paper may be of use to those involved in LDF and HF calculations, GW and other many-body calculations, and classical simulations of charged liquids.

II. VARIATIONAL QMC CALCULATIONS FOR SOLIDS

When performing variational quantum Monte Carlo (VQMC) calculations it is not possible to study an infinite

system. It is, therefore, a finite system which is actually studied. A model electron-electron interaction is used which is designed to mimic the forces on the electrons in the infinite solid. This interaction will be discussed in more detail below.

A. The VQMC method

The VQMC method[17–19] derives from the variational principle. If a system is described by a Hamiltonian $\hat{\mathbf{H}}$ and the energy of the ground state of the system is E_0, then for any reasonable wave function Ψ_{trial},

$$\frac{\int \Psi^*_{\text{trial}} \hat{\mathbf{H}} \Psi_{\text{trial}} d\tau}{\int \Psi^*_{\text{trial}} \Psi_{\text{trial}} d\tau} \geqslant E_0. \tag{1}$$

If $\Psi_{\text{trial}} = \Psi_0$ is the true ground-state wave function for the system then the equality holds; if $\Psi_{\text{trial}} \neq \Psi_0$ then the expectation value of $\hat{\mathbf{H}}$ is greater than E_0 and differs from E_0 by a quantity that is second order in $\Psi_{\text{trial}} - \Psi_0$. It is hoped that if the trial wave function is chosen carefully, taking account of the physics of the system being studied, then the expectation value of $\hat{\mathbf{H}}$ will be a good estimate of E_0.

Our finite HEG system contains N electrons and so the expectation value of the energy is found by evaluating

$$E = \frac{\int \Psi^*(\mathbf{X}) \hat{\mathbf{H}} \Psi(\mathbf{X}) d\mathbf{X}}{\int \Psi^*(\mathbf{X}) \Psi(\mathbf{X}) d\mathbf{X}}, \tag{2}$$

where $\Psi(\mathbf{X}) = \Psi(\mathbf{r}_1, \sigma_1, \mathbf{r}_2, \sigma_2, \ldots, \mathbf{r}_N, \sigma_N)$ is the trial many-body wave function and the integral over $\mathbf{X}$ includes both the $3N$-dimensional spatial integral and the sum over spin indices. Many-dimensional integrals such as this cannot usually be evaluated analytically or by using standard grid based quadratures and so a Monte Carlo method is used. Without loss of generality, $\Psi(\mathbf{X})$ is assumed normalized and Eq. (2) is rewritten as

$$E = \int \frac{1}{\Psi(\mathbf{X})} \hat{\mathbf{H}} \Psi(\mathbf{X}) |\Psi(\mathbf{X})|^2 d\mathbf{X}. \tag{3}$$

$|\Psi(\mathbf{X})|^2$ is now interpreted as a probability distribution and a large but finite set of points is sampled from this probability distribution using, for instance, the Metropolis algorithm.[20] If these points are $\mathbf{X}_1, \ldots \mathbf{X}_M$, then an unbiased statistical estimate of the integral is

$$\frac{1}{M} \sum_{i=1}^{M} \frac{1}{\Psi(\mathbf{X}_i)} \hat{\mathbf{H}} \Psi(\mathbf{X}_i) \tag{4}$$

and the statistical errors in this estimate decay like $M^{-1/2}$ independent of the dimension.[18]

The many-body wave function used in this work is a Slater determinant, as used in the Hartree-Fock approximation, multiplied by a Jastrow factor. The Slater determinant incorporates the effects of particle exchange, and the Jastrow factor introduces correlation. The full many-body wave function takes the following form:

$$\Psi(\mathbf{X}) = \Psi_J(\mathbf{X}) \times D^{\uparrow}(\mathbf{r}_1, \sigma_1, \ldots, \mathbf{r}_{N_\uparrow}, \sigma_{N_\uparrow}) \times D^{\downarrow}(\mathbf{r}_{N_\uparrow+1}, \sigma_{N_\uparrow+1}, \ldots, \mathbf{r}_N, \sigma_N), \tag{5}$$

where $D^{\uparrow}$ and $D^{\downarrow}$ are Slater determinants of spin-up and spin-down one-electron states, respectively, and Ψ_J is the Jastrow factor. This wave function distinguishes between spin-up electrons ($D^{\uparrow}$ is zero unless $\sigma_1, \sigma_2, \ldots, \sigma_{N_\uparrow}$ are all $+1$) and spin-down electrons ($D^{\downarrow}$ is zero unless $\sigma_{N_\uparrow+1}, \sigma_{N_\uparrow+2}, \ldots, \sigma_N$ are all -1) and hence is not antisymmetric under exchange of opposite spin electrons. However, it gives exactly the same energy expectation value as the explicitly antisymmetrized form as long as the Hamiltonian is independent of spin, and the replacement of one large determinant by two smaller ones is numerically efficient.

For the HEG system, the Jastrow factor has the form

$$\Psi_J(\mathbf{X}) = \exp\left(-\frac{1}{2} \sum_{i=1}^{N} \sum_{\substack{j=1 \\ j \neq i}}^{N} u_{\sigma_i \sigma_j}(r_{ij}) \right), \tag{6}$$

where the function $u_{\sigma_i \sigma_j}(r_{ij})$, which depends only on the relative spin of the two particles and their separation, is taken to be

$$u(r) = \frac{A(1 - e^{-r/F})}{r}. \tag{7}$$

The parameters A and F could be determined variationally, but instead we choose them to ensure the correct correlation behavior in the $r \to 0$ and $r \to \infty$ limits.[21] The spin-independent value of A is related to the plasma frequency by

$$A = \frac{1}{\omega_p}, \tag{8}$$

and the spin-dependent value of F is then fixed by the cusp condition at $r = 0$,

$$\left. \frac{du}{dr} \right|_{r=0} = \begin{cases} -1/2 & \text{for opposite spins,} \\ -1/4 & \text{for same spins.} \end{cases} \tag{9}$$

Note that Hartree atomic units are used here and throughout this paper.

In calculations for inhomogeneous systems, the Jastrow factor includes a one-body term $\chi(\mathbf{r})$ as well as the two-body term $u(r)$,

$$\Psi_J(\mathbf{X}) = \exp\left(\sum_{i=1}^{N} \chi(\mathbf{r}_i) - \frac{1}{2} \sum_{i=1}^{N} \sum_{\substack{j=1 \\ j \neq i}}^{N} u_{\sigma_i \sigma_j}(r_{ij}) \right). \tag{10}$$

The one-body term is used to vary the single-particle density to minimize the energy calculated for the system,[17] and to compensate for the fact that the two-body term tends to smooth out the charge density. In the HEG, however, the single-particle density is always uniform and the one-body term is not necessary.

Energies from VQMC calculations for various system sizes are shown in Fig. 1, along with the HF and LDF results for the same systems. The method used to carry out the VQMC calculations closely follows that described by Fahy, Wang, and Louie.[17] After an equilibration period consisting of 2000 moves of all the electrons, averages were accumulated during a further 10^4 to 10^5 N-electron moves (fewer moves are needed for larger system sizes). The one-electron trial moves were sampled from a Gaussian probability distri-

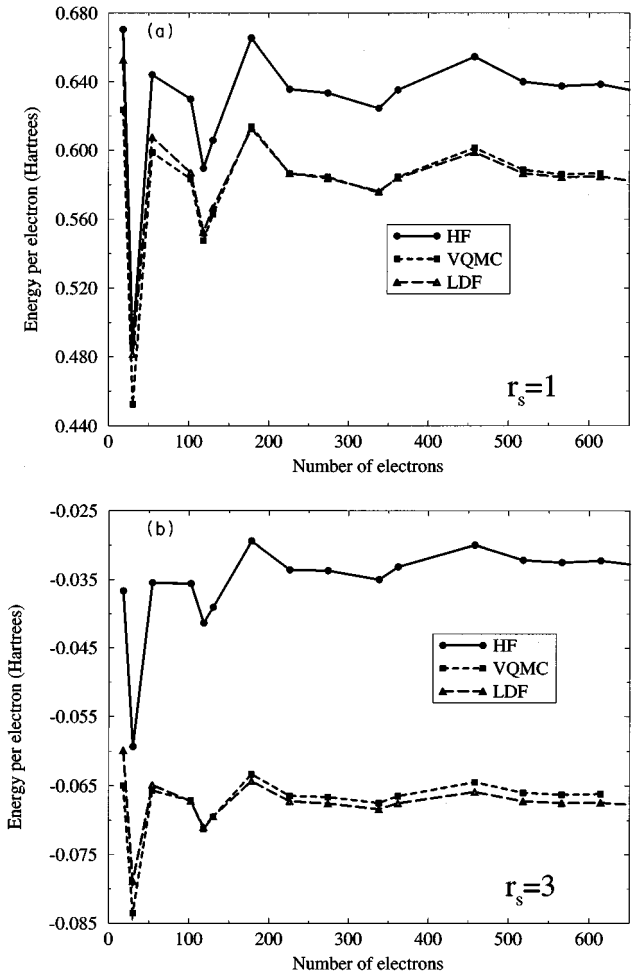

FIG. 1. Total energies per electron calculated for the densities: (a) $r_s=1$, and (b) $r_s=3$. The graphs show the Hartree-Fock (HF), variational quantum Monte Carlo (VQMC), and local-density functional (LDF) energies as functions of the number of electrons in the simulation cell. The HF and VQMC calculations were done using the conventional Ewald interactions between the electrons.

bution of variance 0.5 atomic units. In all of the graphs the statistical errors are smaller than or similar in size to the symbols and so have not been shown explicitly. The density of the HEG is described using the parameter r_s, which is the radius of a sphere whose volume equals the volume per electron so that

$$\frac{1}{\rho}=\frac{4}{3}\pi r_s^3. \tag{11}$$

Two different densities are studied: $r_s=1$ and $r_s=3$ in atomic units.

B. Model electron-electron interaction

We now discuss the form of the electronic Hamiltonian, and in particular the form of the model electron-electron interaction. Consider first an isolated cluster containing N electrons with charges $e=-1$ at positions $\mathbf{r}_i$ and M nuclei with charges Z_α at positions $\mathbf{d}_\alpha$. Within the Born-Oppenheimer approximation, the nuclear positions are frozen and act as parameters in the electronic Hamiltonian,

$$\hat{\mathbf{H}}=-\frac{1}{2}\sum_{i=1}^{N}\nabla_i^2+\mathbf{U}(\mathbf{r}_1,\mathbf{r}_2,\ldots\mathbf{r}_N,\mathbf{d}_1,\mathbf{d}_2,\ldots\mathbf{d}_M). \tag{12}$$

$\mathbf{U}$ is the total electrostatic energy of the cluster and may be calculated in the usual way by summing pairwise $1/r$ interactions. It may also be written in the form

$$\mathbf{U}=\frac{1}{2}\left(\sum_{i=1}^{N}e\bar{\phi}(\mathbf{r}_i)+\sum_{\alpha=1}^{M}Z_\alpha\bar{\phi}(\mathbf{d}_\alpha)\right), \tag{13}$$

where $\bar{\phi}(\mathbf{r})$ is the electrostatic potential at the point $\mathbf{r}$ due to all the charges except the charge at $\mathbf{r}$ itself,

$$\bar{\phi}(\mathbf{r}_i)=\lim_{\mathbf{r}\to\mathbf{r}_i}\left(\phi(\mathbf{r})-\frac{e}{|\mathbf{r}-\mathbf{r}_i|}\right), \tag{14}$$

$$\bar{\phi}(\mathbf{d}_\alpha)=\lim_{\mathbf{r}\to\mathbf{d}_\alpha}\left(\phi(\mathbf{r})-\frac{Z_\alpha}{|\mathbf{r}-\mathbf{d}_\alpha|}\right). \tag{15}$$

$\phi(\mathbf{r})$ is the Coulomb potential due to all the charges and may be obtained by solving Poisson's equation with the boundary condition that the potential tends to zero as $|\mathbf{r}|\to\infty$.

Now consider the electrostatic potential-energy function for a simulation cell in a solid-state QMC calculation. The system being simulated is finite, of course, but in an attempt to make it model an infinite system as well as possible, it is usual to define $\mathbf{U}$ as the Coulomb energy per cell of an infinite periodic array of identical replicas of the simulation cell. This quantity is difficult to evaluate by summing pairwise $1/r$ interactions since the sums are only conditionally convergent.[16] Instead, it is easier to solve Poisson's equation to obtain $\phi(\mathbf{r})$ and then calculate $\mathbf{U}$ from Eqs. (13), (14), and (15), where the sums over i and α now extend over the N electrons and M nuclei in a single simulation cell. Just as for the wave functions in the solution of Schrödinger's equation, it seems natural to insist that the potential obeys periodic boundary conditions, and it is straightforward to show that the solution of Poisson's equation subject to such boundary conditions is unique up to an arbitrary constant. The value of this constant does not affect $\mathbf{U}$ since the simulation cell is charge neutral and so this approach gives an unambiguous result.

It is important to realize that Poisson's equation is solved only within a single simulation cell, with the periodic boundary conditions building in everything about the surroundings (any charges ''outside'' the simulation cell). It is plausible that the use of periodic boundary conditions corresponds to embedding the simulation cell in an infinite periodic array of replicas of that cell, but because of the conditional convergence of the Coulomb sums it is necessary to be very careful about how the limit of infinite system size is taken. We will return to consider this question more carefully in Sec. IV.

In practice, a convenient way to obtain the periodic solution of Poisson's equation is to use the Ewald method.[9,22] This is reasonably efficient for typical QMC simulation cells containing a few hundred point charges, but there is nothing fundamental about the Ewald approach and other methods are more efficient in some cases.[23] Given a simulation cell containing a single unit point charge at position $\mathbf{s}$ along with a uniform canceling background, the Ewald expression for the (unique) periodic potential is

$$\psi(\mathbf{r},\mathbf{s})=\frac{1}{V}\sum_{\mathbf{G}(\neq\mathbf{0})}\frac{\exp[-\pi^2G^2/\kappa^2+2\pi i\mathbf{G}\cdot(\mathbf{r}-\mathbf{s})]}{\pi G^2}-\frac{\pi}{\kappa^2V}+\sum_{\mathbf{R}}\frac{\operatorname{erfc}[\kappa|(\mathbf{r}-\mathbf{s})+R|]}{|(\mathbf{r}-\mathbf{s})+\mathbf{R}|},\tag{16}$$

where κ is an arbitrary positive constant, V is the simulation cell volume, the $\mathbf{R}$ are the lattice vectors for the periodically repeated simulation cell lattice, and the $\mathbf{G}$ are the corresponding reciprocal lattice vectors satisfying $\mathbf{G}\cdot\mathbf{R}=n$ with n an integer (note that the factors of 2π are not included). The value of $\psi(\mathbf{r},\mathbf{s})$ is independent of κ, which can therefore be adjusted to minimize the total computer time required to evaluate the absolutely convergent real and reciprocal space lattice summations. The zero of potential has been chosen so that the average value of $\psi(\mathbf{r},\mathbf{s})$ within the simulation cell is zero. It can be seen that $\psi(\mathbf{r},\mathbf{s})$ depends only on $\mathbf{r}-\mathbf{s}$ and we will occasionally make this explicit by writing $\psi(\mathbf{r}-\mathbf{s})$ in what follows.

The full charge distribution may be obtained by superposing all the point charges and their canceling backgrounds (which sum to zero since the simulation cell is neutral overall), and hence the full potential of the simulation cell is just the sum of the potentials for each charge component,

$$\phi(\mathbf{r})=\sum_{\alpha=1}^{M}Z_\alpha\psi(\mathbf{r},\mathbf{d}_\alpha)+\sum_{j=1}^{N}e\,\psi(\mathbf{r},\mathbf{r}_j).\tag{17}$$

$\bar{\phi}(\mathbf{r}_i)$ then takes the form

$$\bar{\phi}(\mathbf{r}_i)=\sum_{\alpha=1}^{M}Z_\alpha\psi(\mathbf{r}_i,\mathbf{d}_\alpha)+\sum_{\substack{j=1\\j\neq i}}^{N}e\,\psi(\mathbf{r}_i,\mathbf{r}_j)+e\xi,\tag{18}$$

where

$$\begin{aligned}\xi&=\lim_{\mathbf{r}\to\mathbf{s}}\left(\psi(\mathbf{r},\mathbf{s})-\frac{1}{|\mathbf{r}-\mathbf{s}|}\right)\\&=\frac{1}{V}\sum_{\mathbf{G}(\neq\mathbf{0})}\frac{\exp(-\pi^2G^2/\kappa^2)}{\pi G^2}-\frac{\pi}{\kappa^2V}+\sum_{\mathbf{R}(\neq\mathbf{0})}\frac{\operatorname{erfc}(\kappa|\mathbf{R}|)}{|\mathbf{R}|}-\frac{2\kappa}{\sqrt{\pi}}\end{aligned}\tag{19}$$

may be interpreted as the potential at the unit point charge due to its own background and array of images. An analogous expression gives $\bar{\phi}(\mathbf{d}_\alpha)$, and hence the total Coulomb energy per simulation cell is

$$\mathbf{U}=\frac{1}{2}\sum_{i=1}^{N}\sum_{\substack{j=1\\j\neq i}}^{N}e^2\psi(\mathbf{r}_i,\mathbf{r}_j)+\sum_{i=1}^{N}\sum_{\alpha=1}^{M}eZ_\alpha\psi(\mathbf{r}_i,\mathbf{d}_\alpha)+\frac{1}{2}\sum_{\alpha=1}^{M}\sum_{\substack{\beta=1\\\beta\neq\alpha}}^{M}Z_\alpha Z_\beta\psi(\mathbf{d}_\alpha,\mathbf{d}_\beta)+\frac{Ne^2\xi}{2}+\frac{\xi}{2}\sum_{\alpha=1}^{M}Z_\alpha^2.\tag{20}$$

Using the charge neutrality of the simulation cell, $Ne+\sum_{\alpha=1}^{M}Z_\alpha=0$, this may be simplified to

$$\mathbf{U}=\frac{1}{2}\sum_{i=1}^{N}\sum_{\substack{j=1\\j\neq i}}^{N}e^2[\psi(\mathbf{r}_i,\mathbf{r}_j)-\xi]+\sum_{i=1}^{N}\sum_{\alpha=1}^{M}eZ_\alpha[\psi(\mathbf{r}_i,\mathbf{d}_\alpha)-\xi]+\frac{1}{2}\sum_{\alpha=1}^{M}\sum_{\substack{\beta=1\\\beta\neq\alpha}}^{M}Z_\alpha Z_\beta[\psi(\mathbf{d}_\alpha,\mathbf{d}_\beta)-\xi],\tag{21}$$

which is the practical definition of $\mathbf{U}$ that has been used in all solid state QMC calculations until now. It is not the only possible definition, however, and we will show below that it is not the best definition in most cases.

All of the calculations in this paper are for the homogeneous electron gas, which has a uniform canceling background charge in place of the point nuclei. In this case Eq. (18) becomes

$$\bar{\phi}(\mathbf{r}_i)=\sum_{\substack{j=1\\j\neq i}}^{N}e\,\psi(\mathbf{r}_i,\mathbf{r}_j)+e\xi,\tag{22}$$

and the total Coulomb energy per simulation cell is

$$\mathbf{U}=\frac{1}{2}\sum_{i=1}^{N}e\,\bar{\phi}(\mathbf{r}_i)=\frac{1}{2}\sum_{i=1}^{N}\sum_{\substack{j=1\\j\neq i}}^{N}e^2\psi(\mathbf{r}_i,\mathbf{r}_j)+\frac{Ne^2\xi}{2}.\tag{23}$$

The positive background does not appear explicitly because the average value of $\psi(\mathbf{r},\mathbf{s})$ within the simulation cell was chosen to be zero.

III. USUAL CORRECTIONS TO THE VQMC RESULTS

From Fig. 1, it is clear that there are finite-size errors in the VQMC results. These errors far outweigh the statistical errors in the calculation. There are similar finite-size errors in the HF and the LDF results. Since the HF and LDF energies can be calculated exactly for the infinite system simply by improving the k-point sampling, it is possible to find exactly the errors in HF and LDF calculations for finite systems. All the methods appear to have similar size dependence and so the finite-size errors from HF and LDF are often used to try to correct those in VQMC calculations.

A. Finite-size effects in local-density functional theory

In LDF theory,[24,25] the total energy of a solid with given nuclear positions is written as a functional of the electron density,

$$E[\rho(\mathbf{r})]=T[\rho(\mathbf{r})]+E_{\mathrm{xc}}[\rho(\mathbf{r})]+E_{\mathrm{Coulomb}}[\rho(\mathbf{r})+\rho_{\mathrm{nuclear}}(\mathbf{r})],\tag{24}$$

where $T[\rho]$ is the kinetic energy of a fictitious noninteracting electron gas moving in the external potential that makes its density equal to $\rho(\mathbf{r})$, $E_{\mathrm{Coulomb}}[\rho+\rho_{\mathrm{nuclear}}]$ is the Coulomb interaction energy (Hartree energy) of the superposition of

the electronic and nuclear charge densities, and $E_{xc}[\rho]$, known as the exchange-correlation energy, takes care of everything neglected in the first two terms. The nuclear charge density, $\rho_{\text{nuclear}}(\mathbf{r})$, is a superposition of δ functions at the given nuclear positions, but the electronic charge density is smooth. The exchange-correlation energy is approximated using the local density approximation (LDA),

$$E_{xc}[\rho(\mathbf{r})]=\int \epsilon_{xc}(\rho(\mathbf{r}))\rho(\mathbf{r})d\mathbf{r}, \tag{25}$$

where $\epsilon_{xc}(\rho)$ is the exchange-correlation energy per electron of a homogeneous electron gas of density ρ. We use the parametrized form of $\epsilon_{xc}(\rho)$ obtained by Perdew and Zunger[26] from the QMC results of Ceperley and Alder.[6]

In jellium, the one-electron wave functions are plane waves, the LDA is exact, and $E_{\text{Coulomb}}[\rho+\rho_{\text{nuclear}}]$ is zero since the nuclear charges are smeared out into a uniform positive background which exactly cancels the uniform electronic charge density. The energy per electron of an unpolarized jellium simulation cell containing N electrons is therefore given by

$$\epsilon_N=\frac{2}{N}\sum_{\text{occ. }\mathbf{k}}\frac{1}{2}k^2+\epsilon_{xc}(\rho), \tag{26}$$

where the factor of 2 accounts for spin degeneracy. In our QMC calculations the Slater determinant is constructed by doubly occupying each of the lowest $N/2$ k points on the simulation cell reciprocal lattice, so that all the one-electron wave functions have the same periodicity as the simulation cell. If we are to attempt to correct the QMC finite-size errors using LDF results, it is important that the LDF energy for the simulation cell is calculated using this same restricted k-point sampling. (Note that recent work[2] has shown that other wave vectors may also be used in QMC calculations: in most cases the one-electron wave functions should all correspond to the same k point when reduced into the simulation cell Brillouin zone, but that point need not be $\mathbf{k}=\mathbf{0}$. We do not use this extra freedom here.)

The exact exchange-correlation energy per electron in a finite homogeneous electron gas of density ρ depends on the system size, and so it could be argued that we should use a different $\epsilon_{xc}(\rho)$ for each different simulation cell we study. We prefer to use the same $\epsilon_{xc}(\rho)$ in all cases, however, and so our LDF estimate of the jellium exchange-correlation energy per electron does not depend on the system size.

The LDF energy for the infinite system is found by converting the sum in Eq. (26) into an integral over k up to the Fermi wave vector $k_F=(3\pi^2\rho)^{1/3}$,

$$\epsilon_\infty=\frac{1.10495}{r_s^2}+\epsilon_{xc}(\rho). \tag{27}$$

B. Finite-size effects in Hartree-Fock theory

The ground-state energy of the N-electron HEG simulation cell Hamiltonian,

$$\hat{\mathbf{H}}=-\frac{1}{2}\sum_{i=1}^{N}\nabla_i^2+\frac{1}{2}\sum_{i=1}^{N}\sum_{\substack{j=1\\ j\neq i}}^{N}e^2\psi(\mathbf{r}_i,\mathbf{r}_j)+\frac{Ne^2\xi}{2}, \tag{28}$$

may be approximated using HF theory. The periodic (toroidal) boundary conditions are built into the one-electron wave functions, $\langle \mathbf{r},\sigma|\chi_{\mathbf{k},\sigma'}\rangle=\delta_{\sigma,\sigma'}\chi_{\mathbf{k},\sigma'}(\mathbf{r})$ with $\chi_{\mathbf{k},\sigma'}(\mathbf{r})=e^{i\mathbf{k}\cdot\mathbf{r}}/\sqrt{V}$, and all the $\mathbf{k}$ vectors correspond to the point $\mathbf{k}=\mathbf{0}$ when reduced into the simulation cell Brillouin zone. The only unusual feature is the presence of the $\psi(\mathbf{r}_i,\mathbf{r}_j)$ interaction in place of the more familiar $1/r$ Coulomb interaction. This has no effect on the formalism, however, and the total energy is given by the usual HF expression,

$$E=\sum_{\substack{\mathbf{k},\sigma\\ \text{occ.}}}\frac{1}{2}k^2+\frac{Ne^2\xi}{2}+\frac{1}{2}\sum_{\substack{\mathbf{k},\sigma\\ \text{occ.}}}\sum_{\substack{\mathbf{k}',\sigma'\\ \text{occ.}}}\int\int d\mathbf{r}_1 d\mathbf{r}_2|\chi_{\mathbf{k},\sigma}(\mathbf{r}_1)|^2\psi(\mathbf{r}_1,\mathbf{r}_2)|\chi_{\mathbf{k}',\sigma'}(\mathbf{r}_2)|^2$$
$$-\frac{1}{2}\sum_{\substack{\mathbf{k},\sigma\\ \text{occ.}}}\sum_{\substack{\mathbf{k}',\sigma'\\ \text{occ.}}}\delta_{\sigma,\sigma'}\int\int d\mathbf{r}_1 d\mathbf{r}_2\chi^*_{\mathbf{k},\sigma}(\mathbf{r}_2)\chi^*_{\mathbf{k}',\sigma'}(\mathbf{r}_1)\psi(\mathbf{r}_1,\mathbf{r}_2)\chi_{\mathbf{k},\sigma}(\mathbf{r}_1)\chi_{\mathbf{k}',\sigma'}(\mathbf{r}_2), \tag{29}$$

where all integrals are over the volume V of the simulation cell. A similar expression would be obtained for any N-electron Hamiltonian with pairwise interactions plus a constant term.

The $\mathbf{k}=\mathbf{k}'$ exchange term and all the Hartree terms in Eq. (29) vanish because the average value of ψ over the simulation cell is zero, and hence only exchange integrals such as

$$\int\int\frac{d\mathbf{r}_1}{V}\frac{d\mathbf{r}_2}{V}e^{i(\mathbf{k}-\mathbf{k}')\cdot(\mathbf{r}_1-\mathbf{r}_2)}\psi(\mathbf{r}_1,\mathbf{r}_2) \tag{30}$$

with $\mathbf{k}\neq\mathbf{k}'$ are required. These are quite easy to evaluate. First we write

$$\int\frac{d\mathbf{r}_1}{V}e^{i(\mathbf{k}-\mathbf{k}')\cdot(\mathbf{r}_1-\mathbf{r}_2)}\psi(\mathbf{r}_1,\mathbf{r}_2)$$
$$=\int\frac{d\mathbf{r}_1}{V}\left(\frac{-\nabla_1^2e^{i(\mathbf{k}-\mathbf{k}')\cdot(\mathbf{r}_1-\mathbf{r}_2)}}{|\mathbf{k}-\mathbf{k}'|^2}\right)\psi(\mathbf{r}_1,\mathbf{r}_2). \tag{31}$$

Then we use the Hermiticity of the ∇_1^2 operator [assured because both $\psi(\mathbf{r}_1,\mathbf{r}_2)$ and $e^{i(\mathbf{k}-\mathbf{k}')\cdot(\mathbf{r}_1-\mathbf{r}_2)}$ are periodic functions] and the fact that ψ satisfies Poisson's equation within the simulation cell,

$$\nabla_1^2\psi(\mathbf{r}_1,\mathbf{r}_2)=-4\pi[\delta(\mathbf{r}_1-\mathbf{r}_2)+\rho_{\text{back}}], \tag{32}$$

to obtain

$$\int \frac{d\mathbf{r}_1}{V} e^{i(\mathbf{k}-\mathbf{k}')\cdot(\mathbf{r}_1-\mathbf{r}_2)}\psi(\mathbf{r}_1,\mathbf{r}_2)=\frac{4\pi}{V|\mathbf{k}-\mathbf{k}'|^2}. \tag{33}$$

The final expression for the HF ground-state energy per electron of an unpolarized jellium simulation cell containing N electrons is thus

$$\epsilon_N=\frac{2}{N}\sum_{\mathbf{k}\ \text{occ.}}\frac{1}{2}k^2+\frac{e^2\xi}{2}-\frac{1}{N}\sum_{\mathbf{k}\ \text{occ.}}\sum_{\substack{\mathbf{k}'\ \text{occ.}\\ \mathbf{k}\neq\mathbf{k}'}}\frac{4\pi}{V|\mathbf{k}-\mathbf{k}'|^2}. \tag{34}$$

In the limit as the simulation cell becomes very large and $N\to\infty$, the "self-interaction" (ξ) term becomes negligible, the sums over occupied $\mathbf{k}$ vectors become integrals up to k_F, and Eq. (34) gives the usual result,

$$\epsilon_\infty=\frac{1.10495}{r_s^2}-\frac{0.4582}{r_s}. \tag{35}$$

Note that Eq. (33) shows that the Fourier components of $\psi(\mathbf{r})$ are the same as the familiar $4\pi/k^2$ Fourier components of the Coulomb interaction. This does not mean, however, that the complicated Ewald formula for ψ can be replaced by the simple Fourier series,

$$\sum_{\mathbf{k}}\frac{4\pi}{Vk^2}e^{i\mathbf{k}\cdot\mathbf{r}}. \tag{36}$$

The problem is that the Fourier series is conditionally convergent and does not sum to a unique answer; it is only when the product of $\psi(\mathbf{r})$ and some smooth function occurs in an integral over the simulation cell that the replacement is justified.

C. Corrected results for two densities

The LDF and HF energies for an infinite simulation cell with $r_s=1$ are 0.5872 and 0.6468 hartree. When $r_s=3$, the LDF energy is -0.0672 hartree and the HF energy is -0.0299 hartree. The LDF and HF finite-size corrections for a range of different simulation cells are shown in Fig. 2, and the corrected VQMC results are shown in Fig. 3. It can be seen from the graph of finite-size corrections that there is a very slow decay of the HF corrections with increasing system size, which looks as if it must be systematic. Neither method of correction removes all the finite-size errors in the VQMC calculation satisfactorily.

D. Constituent parts of the finite-size error

The VQMC expectation value of the HEG simulation cell Hamiltonian may be written in the form

$$E=T+\frac{Ne^2\xi}{2}+\frac{e^2}{2}\int\int d\mathbf{r}'\,d\mathbf{r}\,\psi(\mathbf{r}',\mathbf{r})n(\mathbf{r}',\mathbf{r}), \tag{37}$$

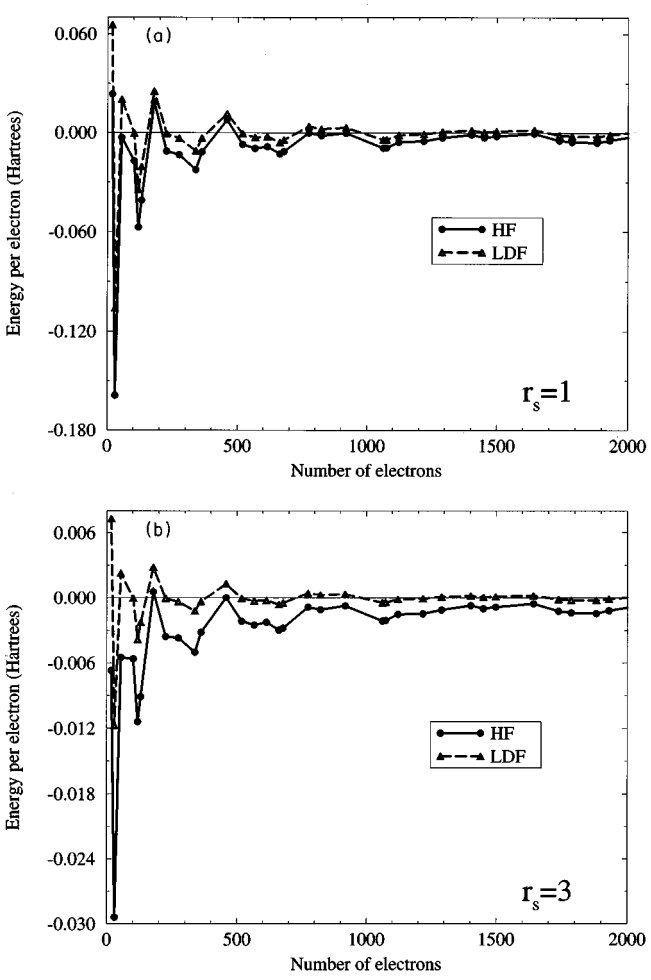

FIG. 2. Finite-size errors in HF and LDF calculations for the densities: (a) $r_s=1$, and (b) $r_s=3$. The finite-size errors are the differences between the energy per electron in a finite system and the energy per electron in an infinite system. The graphs show results for systems containing up to 2000 electrons. The HF errors were calculated using the conventional Ewald Hamiltonian and decay very slowly with system size.

where T is the kinetic energy expectation value, the $\mathbf{r}$ and $\mathbf{r}'$ integrals both extend over the simulation cell, and $n(\mathbf{r}',\mathbf{r})$ is the (diagonal part of the) two-electron density matrix,

$$n(\mathbf{r}',\mathbf{r})=\int d\mathbf{X}|\Psi(\mathbf{X})|^2\sum_{\substack{i,j=1\\ j\neq i}}^{N}\delta(\mathbf{r}'-\mathbf{r}_i)\,\delta(\mathbf{r}-\mathbf{r}_j). \tag{38}$$

When $|\mathbf{r}'-\mathbf{r}|$ is large, $n(\mathbf{r}',\mathbf{r})$ tends to $n(\mathbf{r}')n(\mathbf{r})$, where

$$n(\mathbf{r})=\int d\mathbf{X}|\Psi(\mathbf{X})|^2\sum_{i=1}^{N}\delta(\mathbf{r}-\mathbf{r}_i) \tag{39}$$

is the electron density. For small $|\mathbf{r}'-\mathbf{r}|$, however, $n(\mathbf{r}',\mathbf{r})$ is suppressed because of Coulomb repulsion and (for spin parallel electrons) the Pauli principle. The suppression of the density at $\mathbf{r}'$ due to the presence of an electron at $\mathbf{r}$ is conveniently described in terms of the exchange-correlation hole, $n_{\text{xc}}(\mathbf{r}',\mathbf{r})$, defined via

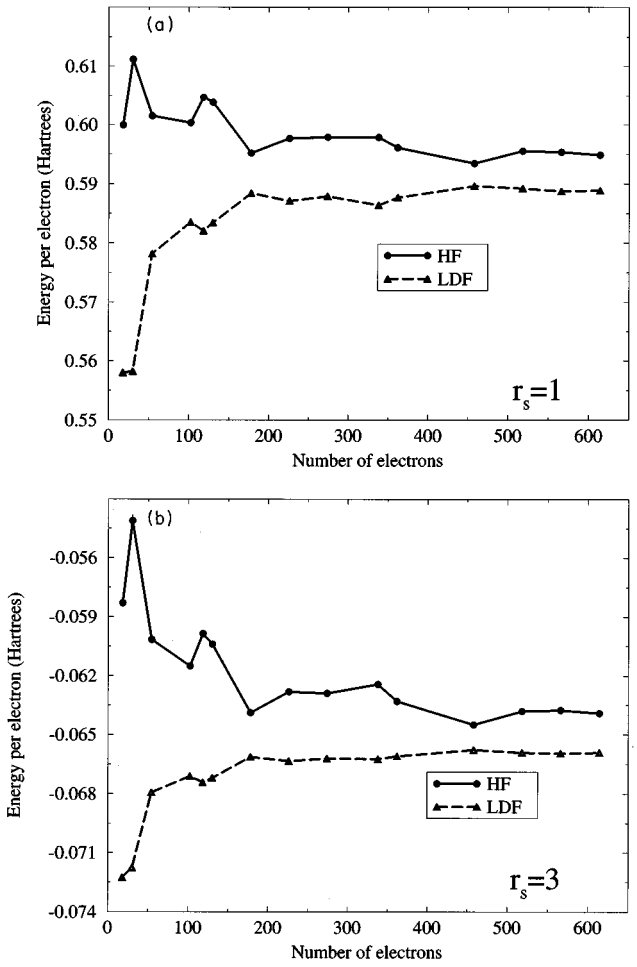

FIG. 3. VQMC results corrected using the finite-size errors from HF and LDF calculations. The VQMC and HF results were obtained using the conventional Ewald simulation cell Hamiltonian. Results are for systems containing from 18 to 614 electrons and for the densities (a) $r_s=1$ and (b) $r_s=3$. Even for large system sizes the corrected VQMC results do not converge.

$$n(\mathbf{r}',\mathbf{r})=n(\mathbf{r}')n(\mathbf{r})+n_{\mathrm{xc}}(\mathbf{r}',\mathbf{r})n(\mathbf{r}). \tag{40}$$

It is easy to show that

$$\int_{\mathrm{cell}} d\mathbf{r}'\, n_{\mathrm{xc}}(\mathbf{r}',\mathbf{r})=-1 \tag{41}$$

irrespective of the size of the system and so the full exchange-correlation hole containing charge $|e|$ is always ''squashed in'' to even the smallest simulation cell.

Since the average value of $\psi(\mathbf{r}',\mathbf{r})$ over the simulation cell is zero and the density is constant in jellium, the total energy becomes

$$E=T+\frac{e^2}{2}\int\int d\mathbf{r}'\,d\mathbf{r}\, n_{\mathrm{xc}}(\mathbf{r}',\mathbf{r})[\psi(\mathbf{r}',\mathbf{r})-\xi]n(\mathbf{r})$$

$$=T+U_{\mathrm{xc}}, \tag{42}$$

where U_{xc} is the exchange-correlation energy. The interpretation of this equation is clear: the exchange-correlation energy arises from the interaction of the electron at $\mathbf{r}$ with the unit positive charge distribution that makes up its exchange-correlation hole. A similar result holds in an infinite jellium system, of course, except that then the $1/|\mathbf{r}'-\mathbf{r}|$ Coulomb interaction replaces the effective $\psi(\mathbf{r}',\mathbf{r})-\xi$ interaction. Note that

$$\psi(\mathbf{r}',\mathbf{r})\sim\frac{1}{|\mathbf{r}'-\mathbf{r}|}+\xi+\cdots \tag{43}$$

for small $|\mathbf{r}'-\mathbf{r}|$, and so the effective interaction does at least resemble the Coulomb interaction near the origin. Note also that although the exchange-correlation hole in an infinite jellium is exactly spherical, the hole in a finite simulation cell is not.

If the kinetic energy expectation value is split up into a one-electron part, T_{1e}, as in density functional theory, and a many-electron part, T_{me}, then the full VQMC energy is

$$E=T_{1e}+T_{\mathrm{me}}+U_{\mathrm{xc}} \tag{44}$$

$$=T_{1e}+\tilde{U}_{\mathrm{xc}}, \tag{45}$$

where $\tilde{U}_{\mathrm{xc}}$ is the exchange-correlation energy as used in density functional theory and is defined by Eq. (45). $\tilde{U}_{\mathrm{xc}}$ is not the same as U_{xc} but may also be expressed as an integral over an exchange-correlation hole.[24,25] The form of the integral is the same as in Eq. (42), but now it is necessary to use an averaged exchange-correlation hole accumulated as the electron-electron interactions are slowly ''switched on.''

When VQMC results are finite-size corrected using LDF results it is ΔT_{1e}, the error in the one-electron kinetic energy, which is being corrected. The LDF exchange-correlation energy is independent of the cell size and so ΔT_{me}, the error in the many-electron part of the kinetic energy, and ΔU_{xc}, the error in the exchange-correlation energy, remain.

When HF results are used, both ΔT_{1e} and ΔU_x, the error due to the exchange energy, are corrected. The exchange energy arises from the effective $[\psi(\mathbf{r}',\mathbf{r})-\xi]$ interaction of an electron with its exchange hole. Like the exchange-correlation hole, the exchange hole contains charge $|e|$, and so any difference between ΔU_x and ΔU_{xc} must be entirely attributable to the different shapes of the two holes.

Figures 4 and 5 show the exchange and exchange-correlation holes in jellium as functions of the size of the simulation cell. The calculations were carried out using our QMC program and the statistical errors are visible near $r=0$. It can be seen that both the exchange hole and the exchange-correlation hole are short ranged and hardly change at all with simulation cell size. [The exchange hole decays like $1/(k_F r)^4$ in an infinite jellium but the large r tail is small and oscillatory and contributes little to the exchange energy.] For this reason, one might expect the finite-size errors in U_x and U_{xc} (and presumably also in $\tilde{U}_{\mathrm{xc}}$) to converge very quickly to zero with increasing system size, and hence both the HF and LDF corrected VQMC results should also converge quickly. However, it is clear from Fig. 3 that the errors do not converge quickly and that they still appear to have a systematic nature. This suggests that the problem must lie with the slow convergence of the effective interaction, $\psi(\mathbf{r}',\mathbf{r})-\xi$, to the Coulomb $1/|\mathbf{r}'-\mathbf{r}|$ form. It seems

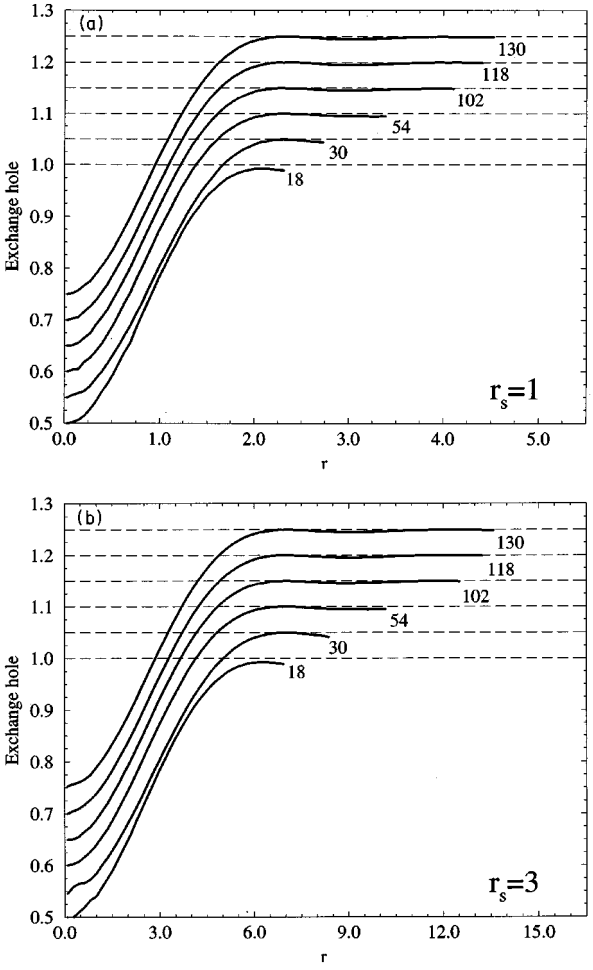

FIG. 4. Spherically averaged exchange hole as calculated using the VQMC program for the densities (a) $r_s=1$ and (b) $r_s=3$. Each figure shows the exchange hole for systems containing various numbers of electrons. The graphs for different system sizes have been offset by multiples of 0.05 for clarity; they all tend to 1 at large r and are equal to 0.5 at $r=0$.

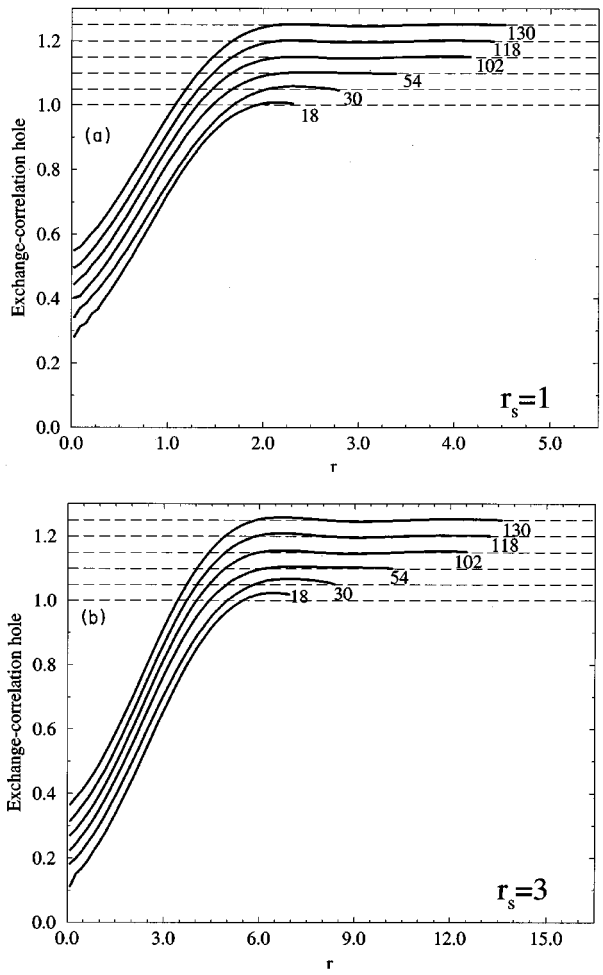

FIG. 5. Spherically averaged exchange-correlation hole calculated using the VQMC program for the densities (a) $r_s=1$ and (b) $r_s=3$. Each figure shows the exchange-correlation hole for systems containing various numbers of electrons. The graphs for different system sizes have been offset by multiples of 0.05 for clarity; they all tend to 1 at large r.

that the slowly decaying finite-size errors are caused by the form of the simulation cell Hamiltonian rather than the form of the trial wave function.

IV. COULOMB ENERGIES AND POTENTIALS IN PERIODIC SOLIDS

A. Introductory discussion

Since the long-ranged finite-size errors seem to be a consequence of the form of the simulation cell Hamiltonian, let us look again at the definition of the simulation cell Coulomb energy. The only sensible criterion to use in choosing the form of **U** is to try to mimic the interactions in a real solid as well as possible. The main problem is the obvious one: a real solid is a macroscopic (but finite) cluster containing an enormous number of electrons, whereas a QMC simulation cell contains only a few hundred.

The standard solution to this problem is to make **U** the Coulomb energy per simulation cell of an infinite periodic array of identical copies of that cell. This approach suffers from problems of its own, however, arising from the infinite range of the correlations between electronic positions in the periodic array. Even when the simulation cell has no dipole moment on average, almost every configuration, **X**, sampled during the QMC run will have a nonzero dipole moment. This moment will be mirrored in every other simulation cell of the infinite periodic array, and the interactions between all these dipoles may give rise to an unphysical contribution to the potential energy of the configuration. There will also be contributions from interactions involving higher multipole moments, but these decay more quickly as the simulation cell size increases and so are less important. In a real solid, the central dipole induces much weaker dipoles in surrounding regions (hence the van der Waals interaction), but these die off very rapidly with distance.

Even if we accept the use of a periodic array of copies of the simulation cell, there still remains the practical difficulty of calculating the potential energy. We cannot simply sum $1/r$ interactions as in a finite cluster since the long range of the Coulomb interaction means that such sums are only conditionally convergent; the answer obtained depends on the order of summation and it is hard to know which order is the appropriate one.

At first sight, this conditional convergence difficulty is surprising. We know that the only effect of the surfaces on the electrostatic potential deep inside a real piece of solid is a constant shift due to the surface dipole layer. The value of this constant does not affect the electrostatic energy per unit volume as long as the solid is charge neutral on average and so **U** is independent of the shape of the piece of solid. This unique value of **U** is clearly the right one to associate with the total electrostatic energy per simulation cell and is in principle straightforward to evaluate: one simply chooses a sensible cluster shape and sums $1/r$ interactions for a sequence of bigger and bigger clusters of that shape until the calculated values of **U** converge.

The fact that the final result is independent of the shape of the cluster relies, however, on a statistical cancellation of the contributions from far regions of the solid: some distant regions have an excess of positive charge and some of negative charge, but the fields they produce cancel out on average because the charges are randomly distributed. The cancellation must be very efficient since at any given time most of the cells in the cluster will have nonzero monopole moments as well as nonzero dipole and higher multipole moments.

Unfortunately, the cancellation does not work for the periodic array of *identical* replicas of the simulation cell used to define the potential in a QMC calculation. Although the cells have no charge (i.e., no monopole moment), they usually have a nonzero dipole moment and so the array of identical replicas has a nonzero dipole moment per unit volume. The surfaces of any finite cluster are therefore covered with a layer of polarization charge, and the value of **U** is affected by the resulting depolarization fields, which are well known to depend on the shape of the cluster.[27] Clusters of different shapes give different values for **U** even in the limit as the cluster size tends to infinity, and it is not clear which shape is best. Ferromagnets show a similar dependence of total energy on cluster shape (although large clusters avoid depolarization fields by splitting up into domains) and the physics is of course well understood. We will come back to consider this problem in more detail below.

In Sec. II, the conditional convergence problem led us to calculate **U** using a different approach, which at least gives an unambiguous result. Poisson's equation was solved within the simulation cell using periodic boundary conditions, and **U** was then obtained from Eq. (13), where the sums over i and α extended over all electrons and nuclei in the simulation cell. This approach does not rely on the construction of an artificial periodic lattice of replicas of the simulation cell since all the information about the ''surroundings'' is built into the periodic boundary conditions.

For smooth charge distributions, Poisson's equation is most easily solved by Fourier transformation. The charge density and potential are expanded as Fourier series with components at spatial frequencies given by the reciprocal lattice vectors of the simulation cell,

$$\rho(\mathbf{r})=\sum_{\mathbf{G}}\ \rho_{\mathbf{G}}e^{2\pi i\mathbf{G}\cdot\mathbf{r}}, \tag{46}$$

$$\phi(\mathbf{r})=\sum_{\mathbf{G}}\ \phi_{\mathbf{G}}e^{2\pi i\mathbf{G}\cdot\mathbf{r}}, \tag{47}$$

and these expansions are substituted into Poisson's equation to obtain

$$(2\pi G)^2\phi_{\mathbf{G}}=4\pi\rho_{\mathbf{G}}. \tag{48}$$

The $\mathbf{G}=\mathbf{0}$ equation is not soluble unless $\rho_{\mathbf{G}=\mathbf{0}}=0$, and hence the simulation cell must be charge neutral. As long as this condition is satisfied, however, $\phi_{\mathbf{G}=\mathbf{0}}$ is arbitrary and all other Fourier components of the potential are uniquely determined. The arbitrary average value of the potential, $\phi_{\mathbf{G}=\mathbf{0}}$, cancels from the expression for **U** and is usually set equal to zero for convenience.

The charge densities for which we wish to evaluate **U** during solid-state QMC calculations are made up of δ-function point charges and so the Fourier series in Eq. (46) does not converge. The required periodic solution of Poisson's equation may now be found using the Ewald method (see Sec. II and Ref. 9), however, and **U** can still be obtained from Eq. (13). The uniqueness of the periodic solution of Poisson's equation may now be demonstrated by supposing there are two different periodic solutions, $\phi_1(\mathbf{r})$ and $\phi_2(\mathbf{r})$, and considering the difference between them, $\phi(\mathbf{r})=\phi_1(\mathbf{r})-\phi_2(\mathbf{r})$, which is also periodic but satisfies Laplace's equation, $\nabla^2\phi(\mathbf{r})=0$. If $\phi(\mathbf{r})$ is anything other than a constant then it must reach both maximum and minimum values at points within the simulation cell and so cannot satisfy Laplace's equation everywhere. We therefore conclude that $\phi_1(\mathbf{r})$ and $\phi_2(\mathbf{r})$ differ by at most an arbitrary constant.

B. Ewald potentials and cluster potentials

The Ewald approach to the definition of **U** is clearly sensible but the physical situation to which it corresponds is not clear. It seems plausible that the use of periodic boundary conditions is equivalent to embedding the simulation cell in an infinite lattice of identical replicas of that cell, but we have already explained that finite clusters of different shapes have different electrostatics even in the limit as the cluster size tends to infinity and so it is not clear exactly what this means. The question was settled (although only for ionic systems and simple cubic simulation cells) by de Leeuw, Perram, and Smith,[16] using an approach that is quite rigorous but highly mathematical and far from transparent (see Ref. 22 for a concise summary of the results). In Appendix A we show how this approach may be generalized to arbitrary lattices and charge distributions with continuous components such as the background charge in jellium. In this section, however, we rederive the main results using more physical arguments.

We start by considering the Coulomb potential inside a large spherical cluster of simulation cells and finding out how it differs from the Ewald potential. Because of the long range of the Coulomb interaction, it is necessary to be very precise about the shape of the cluster boundary: a radius R_c is chosen and all simulation cells centered on lattice vectors **R** with $|\mathbf{R}|\leqslant R_c$ are included in the cluster. Note that if a cell is included in the cluster then *all* charges within that cell are included, even though some of them may be a little further than R_c from the origin.

Now refer to Fig. 6 and consider the values of the potential at the points **r** and $\mathbf{r}+\mathbf{A}$, where **A** is one of the three

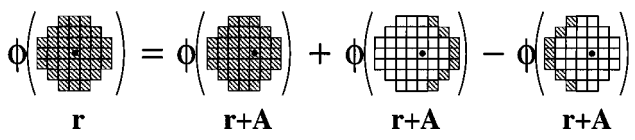

FIG. 6. The contributions to the difference in potential between points $\mathbf{r}$ and $\mathbf{r}+\mathbf{A}$ when cluster boundary conditions are imposed on Poisson's equation. $\mathbf{A}$ is a simulation cell lattice vector and $\mathbf{r}$ is an arbitrary point near the center of the cluster.

primitive vectors of the simulation cell lattice. Both the Ewald and cluster potentials in any given cell may be obtained by solving Poisson's equation within that cell, but the two potentials are not the same because the boundary conditions are different. We will work out the difference between $\phi(\mathbf{r})$ and $\phi(\mathbf{r}+\mathbf{A})$ for an arbitrary point $\mathbf{r}$ deep within the spherical cluster, and hence determine the boundary conditions obeyed by the cluster potential and how it differs from the periodic Ewald potential.

Since the spherical cluster is finite, both $\phi(\mathbf{r})$ and $\phi(\mathbf{r}+\mathbf{A})$ can be obtained by summing Coulomb $1/r$ contributions from all the other charges in the cluster. Almost all the terms in the two sums are the same, but $\phi(\mathbf{r})$ contains extra contributions from a shell of cells on the hemispherical surface of the cluster centered around the $\mathbf{A}$ direction, and $\phi(\mathbf{r}+\mathbf{A})$ contains extra contributions from the hemispherical shell of cells centered around the $-\mathbf{A}$ direction. The difference between $\phi(\mathbf{r})$ and $\phi(\mathbf{r}+\mathbf{A})$ comes entirely from the single layer of cells on the surface of the large spherical cluster. When viewed along the $\mathbf{A}$ direction, the projection of all the cells in either of the two hemispherical shells exactly covers the projection of the sphere, and so it is straightforward to find the number of cells in the surface layer per unit area of the sphere. If d^2S is an element of surface area on the sphere lying at an angle θ to the $\mathbf{A}$ direction, then the corresponding projected area is $|\cos\theta|\, d^2S$. The projected area of any single unit cell is $V/|\mathbf{A}|$ and hence the number of surface cells in the area d^2S is given by

$$c(\theta)d^2S=\frac{|\cos\theta|d^2S}{V/|\mathbf{A}|}=\frac{|\mathbf{A}\,\cos\theta|}{V}d^2S. \tag{49}$$

Although the cells in the surface layer are all charge neutral, they almost always have nonzero dipole and higher multipole moments. The cell at $\mathbf{R}$ with dipole moment $\mathbf{p}$ therefore produces a potential

$$\phi_{\mathbf{R}}(\mathbf{r})=\frac{-\mathbf{p}\cdot(\mathbf{R}-\mathbf{r})}{|\mathbf{R}-\mathbf{r}|^3}+O\left(\frac{1}{(R-r)^3}\right) \tag{50}$$

at the point $\mathbf{r}$. (Note that in an infinite periodic system, the dipole moment of the unit cell,

$$\mathbf{p}=\sum_{i=1}^{N} e\mathbf{r}_i+\sum_{\alpha=1}^{M} Z_\alpha \mathbf{d}_\alpha, \tag{51}$$

depends on where you draw the cell boundaries and so cannot be uniquely defined. In our case, however, $\mathbf{p}$ means the dipole moment of the simulation cell used in the QMC calculation and there is no ambiguity.) Given that the cluster is large, and assuming that $\mathbf{r}$ is not too close to the surface, the sums of dipolar contributions giving the difference between $\phi(\mathbf{r})$ and $\phi(\mathbf{r}+\mathbf{A})$ may be replaced by integrals,

$$\begin{aligned}\phi(\mathbf{r}+\mathbf{A})-\phi(\mathbf{r})=&\int_{\phi=0}^{2\pi}\int_{\theta=\pi/2}^{\pi}\frac{-\mathbf{p}\cdot(\mathbf{R}-\mathbf{r})}{|\mathbf{R}-\mathbf{r}|^3}\,c(\theta)d^2S_{\mathbf{R}}\\&-\int_{\phi=0}^{2\pi}\int_{\theta=0}^{\pi/2}\frac{-\mathbf{p}\cdot(\mathbf{R}-\mathbf{r})}{|\mathbf{R}-\mathbf{r}|^3}c(\theta)d^2S_{\mathbf{R}}\\&+O\left(\frac{1}{R_c}\right),\end{aligned} \tag{52}$$

where the points $\mathbf{R}=(R_c,\theta,\phi)$ lie on the spherical surface of the cluster, and $d^2S_{\mathbf{R}}$ is the element of surface area. Ignoring the $O(1/R_c)$ contributions and combining the two integrals gives

$$\begin{aligned}\phi(\mathbf{r}+\mathbf{A})-\phi(\mathbf{r})=&\frac{|\mathbf{A}|}{V}\oint\frac{\mathbf{p}\cdot(\mathbf{R}-\mathbf{r})}{|\mathbf{R}-\mathbf{r}|^3}\cos\theta d^2S_{\mathbf{R}}\\=&\frac{|\mathbf{A}|}{V}(\mathbf{p}\cdot\nabla_{\mathbf{r}})\oint\frac{\cos\theta}{|\mathbf{R}-\mathbf{r}|}d^2S_{\mathbf{R}}.\end{aligned} \tag{53}$$

The remaining integral can be evaluated as explained in Ref. 28 and hence one obtains

$$\phi(\mathbf{r}+\mathbf{A})=\phi(\mathbf{r})+\frac{4\pi\mathbf{p}\cdot\mathbf{A}}{3V}. \tag{54}$$

Equation (54) is the main result of this section. It shows that the cluster Coulomb potential is not periodic and so is not the same as the Ewald potential. However, given that $\phi_{\text{Ewald}}(\mathbf{r})$ is a periodic solution of Poisson's equation, it follows that the function

$$\phi_{\text{cluster}}(\mathbf{r})=\phi_{\text{Ewald}}(\mathbf{r})+\frac{4\pi\mathbf{p}\cdot\mathbf{r}}{3V}, \tag{55}$$

satisfies Poisson's equation for the same charge distribution but with the boundary conditions specified in Eq. (54). A simple adaptation of the uniqueness proof for periodic boundary conditions shows that this solution of Poisson's equation is also unique, and so $\phi_{\text{cluster}}(\mathbf{r})$ must indeed be the Coulomb potential of the cluster to within an arbitrary constant.

Equation (55) applies both for a system of point charges and for jellium as long as the appropriate Ewald potential is used, but note that $\mathbf{p}$ is the full dipole moment of the simulation cell and so includes the dipole moment of the ions or background charge distribution as well as the dipole moment of the electrons. It is only when the origin of coordinates is chosen to make the dipole moment of the ions or background equal to zero that the electronic dipole moment alone may be used.

The fact that the difference between ϕ_{Ewald} and ϕ_{cluster} is a uniform electric field should not be surprising. The sum of dipolar contributions that gives the value of the potential at the center of the cluster is not absolutely convergent and so the result may depend on the cluster shape. The same applies to the sum of first derivatives of dipole potentials that gives the electric field, but sums of second derivatives of dipole

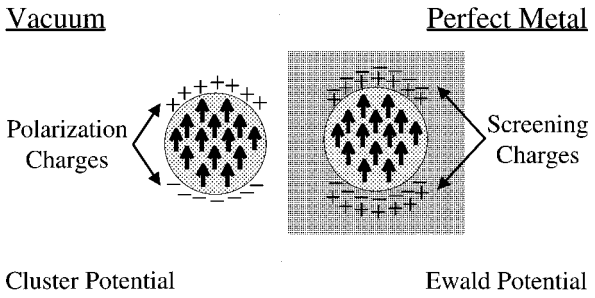

FIG. 7. Polarization charges and screening charges induced when a large cluster of simulation cells is embedded in either a vacuum or a perfect metal. The differences between the two macroscopic charge distributions account for the differences between the cluster potential and the Ewald potential.

potentials *are* absolutely convergent and so gradients and higher derivatives of the electric field are independent of cluster shape.

The extra electric field,

$$\mathbf{E}=-\frac{4\pi\mathbf{p}}{3V}, \tag{56}$$

in Eq. (55) has a simple physical interpretation in terms of macroscopic electrostatics. Figure 7 shows a sphere with uniform dipole moment per unit volume, $\mathbf{P}=\mathbf{p}/V$. The charge density within the sphere is everywhere zero and so all the field comes from the surface charge per unit area, $\mathbf{P}\cdot\mathbf{n}$, where $\mathbf{n}$ is the unit outward normal to the surface. The electric field at the center of the sphere due to this surface charge distribution is easily evaluated and is exactly that of Eq. (56). The extra electric field that distinguishes the cluster potential from the Ewald potential is therefore nothing more than the depolarization field, which is present in the cluster potential but not in the Ewald potential. Once this is understood, it is easy to devise a physical system for which the periodic Ewald potential is exact. If a large spherical cluster of identical simulation cells is embedded in a perfect metal, the surface charges will be perfectly screened, the depolarization field will be zero, and the Ewald potential will be the exact potential.

The expression for the Coulomb energy of the cluster may be found by combining Eqs. (55) and (13), where the sums over i and α run over all electrons and nuclei in the cluster. The average value of the potential varies from cell to cell because of the depolarization field term, but all the cells are charge neutral and so contribute the same amount to the total energy. The neglected $O(1/R_c)$ terms alter the potential near the surface of the cluster, of course, but the proportion of simulation cells affected tends to zero as the cluster size tends to infinity, and as expected the cluster energy becomes an extensive quantity. The energy per simulation cell is then

$$U_{\text{cluster}}=U_{\text{Ewald}}+\frac{2\pi|\mathbf{p}|^2}{3V}. \tag{57}$$

Given that the simulation cell is neutral and contains charges (electronic and nuclear) q_k at positions $\mathbf{r}_k$, it is easy to show that

$$|\mathbf{p}|^2=-\frac{1}{2}\sum_i\sum_{(j\neq i)}^{\ }q_iq_j|\mathbf{r}_i-\mathbf{r}_j|^2, \tag{58}$$

and so the dipole term may be viewed as the result of an extra quadratic interaction between charges. This means that if the modified interaction,

$$\psi_{\text{cluster}}(\mathbf{r},\mathbf{s})=\psi(\mathbf{r},\mathbf{s})-\frac{2\pi}{3V}|\mathbf{r}-\mathbf{s}|^2, \tag{59}$$

is used in place of $\psi(\mathbf{r},\mathbf{s})$, then the standard Ewald formula, Eq. (21), for the total energy of a simulation cell containing electrons and ions gives the cluster energy instead. [Note, however, that the average value of ψ_{cluster} is not zero and so the expression for the cluster energy of a jellium simulation cell,

$$\begin{aligned}\mathbf{U}_{\text{cluster}}=&\frac{1}{2}\sum_{i=1}^{N}\sum_{\substack{j=1\\ j\neq i}}^{N}e^2\psi_{\text{cluster}}(\mathbf{r}_i,\mathbf{r}_j)+\frac{Ne^2\xi}{2}\\ &+\frac{eN}{V}\sum_i\int d^3r\left(-\frac{2\pi}{3V}|\mathbf{r}_i-\mathbf{r}|^2\right)\\ &+\frac{N^2}{2V^2}\int d^3r\int d^3r'\left(-\frac{2\pi}{3V}|\mathbf{r}-\mathbf{r}'|^2\right),\end{aligned} \tag{60}$$

involves background terms. It is not correct simply to replace ψ by ψ_{cluster} in Eq. (23).]

V. COULOMB ENERGIES AND POTENTIALS IN QMC CALCULATIONS

In Sec. III we discussed the constituent parts of the finite-size error in a VQMC calculation. We explained that the error in the one-electron kinetic energy, ΔT_{1e}, is completely removed if LDF corrections are used, and so the residual error is $\Delta\tilde{U}_{\text{xc}}=\Delta T_{\text{me}}+\Delta U_{\text{xc}}$. Like the true exchange-correlation hole shown in Fig. 5, the ''averaged'' exchange-correlation hole that determines $\tilde{U}_{\text{xc}}$ is expected to be short ranged and to converge rapidly with increasing cell size. The existence of significant residual errors for large simulation cells with well converged exchange-correlation holes shows that the problem must lie in the choice of simulation cell Hamiltonian rather than the choice of trial wave function.

In Sec. IV we explained that the Coulomb potential in a large cluster of identical simulation cells depends on the shape of the cluster and the properties of the medium in which the cluster is embedded. The periodic boundary conditions assumed in the calculation of the Ewald potential (which amount to embedding a large spherical cluster in a perfect metal) seem physically sensible, but they are not the only sensible choice. Perhaps the residual finite-size errors will be smaller if the model electron-electron interactions used in the simulation cell Hamiltonian correspond to a different choice of boundary conditions?

To address this question, we return to the expression for the exchange-correlation energy,

$$U_{\text{xc}}=\frac{e^2}{2}\int\int d\mathbf{r}'\,d\mathbf{r}\,n_{\text{xc}}(\mathbf{r}',\mathbf{r})[\psi(\mathbf{r}',\mathbf{r})-\xi]n(\mathbf{r}). \tag{61}$$

We can gain a better understanding of this expression by considering a simulation cell containing just two charges, a unit negative charge at $\mathbf{r}$ and a unit positive charge at $\mathbf{r}'$. A simple application of Eq. (21) shows that the Ewald energy of this two-charge cell is $U_2(\mathbf{r}',\mathbf{r})=\xi-\psi(\mathbf{r}',\mathbf{r})$ and so Eq. (61) can be rewritten as

$$U_{\mathrm{xc}}=-\frac{e^2}{2}\int\int d\mathbf{r}'d\mathbf{r}n_{\mathrm{xc}}(\mathbf{r}',\mathbf{r})U_2(\mathbf{r}',\mathbf{r})n(\mathbf{r}). \quad (62)$$

Given that n_{xc} settles down fairly rapidly to its asymptotic form as the size of the simulation cell increases, the main finite-size errors must arise from the slow convergence of $U_2(\mathbf{r}',\mathbf{r})$ to the $-1/|\mathbf{r}'-\mathbf{r}|$ Coulomb interaction. Furthermore, since the exchange-correlation hole charge density decreases rapidly to zero as $\mathbf{r}'-\mathbf{r}$ increases, it is only the rate of convergence when $\mathbf{r}'-\mathbf{r}$ is small that matters. We can (and will) address this convergence question purely mathematically, but given the understanding of the Ewald potential gained in the previous section, it is more illuminating to start by making a physical argument.

Imagine a large spherical cluster of copies of the ''two-charge'' simulation cell embedded in a perfect metal. According to our earlier discussion, $U_2(\mathbf{r}',\mathbf{r})$ is the Coulomb energy of the central cell in this cluster. We can therefore obtain U_2 by summing Coulomb contributions from all the other charges in the cluster and from the metallic screening charges that build up on the cluster surface. U_2 is a periodic function of the distance between the two charges and so is unchanged when the two charges are picked up and moved together through the simulation cell. It turns out, however, that the argument is easier to follow when both charges are near the center of the cell and this will be assumed from now on.

The first contribution to $U_2(\mathbf{r}',\mathbf{r})$ arises from the interaction of the two charges in the central simulation cell. This term is just the $-1/|\mathbf{r}-\mathbf{r}'|$ Coulomb energy and so any contributions from the rest of the cluster may be regarded as finite-size errors. The potentials from other cells may be represented as multipole expansions, but only the dipole terms matter because the distance between the two charges is much smaller than the shortest translation vector of the simulation cell lattice (the exchange-correlation hole decays so rapidly that the form of the interaction is irrelevant when the two charges are further apart). The finite-size error due to the other cells in the cluster may therefore be approximated as a sum of dipole-dipole interaction energies.

Dipole-dipole interactions decay like $1/R^3$ and so lattice dipole sums are conditionally convergent, but here the sum runs over all the cells in the large but finite spherical cluster and so is well defined. Furthermore, a straightforward symmetry argument[27] shows that the sum is zero in any lattice with cubic symmetry. Our QMC calculations used face-centered cubic simulation cells and so the dipole sum is zero and the leading nonzero contributions to $U_2(\mathbf{r}',\mathbf{r})$ arise from higher multipole moments. These contributions must decrease at least as fast as $1/L^5$ and so cannot explain the observed long-range $(1/L^3)$ finite-size errors.

The remaining term present in $U_2(\mathbf{r}',\mathbf{r})$ is due to the metallic charges that flow to screen the polarization charges on the surface of the cluster. (The polarization charges themselves simply provide a convenient macroscopic description of the effects of the microscopic charges in the cluster of cells and hence have already been included in the dipole sum.) We have already explained that these screening charges give rise to a uniform electric field, $\mathbf{E}=4\pi\mathbf{p}/3V=4\pi(\mathbf{r}'-\mathbf{r})/3V$, within the cluster, and hence produce what amounts to a repulsive force, $\mathbf{F}_{\mathrm{screening}}=4\pi(\mathbf{r}'-\mathbf{r})/3V$, between the two unit charges in the central simulation cell. This adds an extra quadratic term,

$$U_{\mathrm{screening}}=-\frac{2\pi|\mathbf{r}'-\mathbf{r}|^2}{3V}, \quad (63)$$

to U_2.

How does this ''screening'' term affect the exchange-correlation energy? To simplify the argument, we approximate by using the exchange hole in place of the exchange-correlation hole in Eq. (62), and assume that the simulation cell is large enough for the exchange hole to be the same as in an infinite jellium,

$$n_{\mathrm{x}}(\mathbf{r}',\mathbf{r})=\frac{1}{r_s^3}f(|\mathbf{r}'-\mathbf{r}|/r_s), \quad (64)$$

where f is a known function.[29] The charge density, $n(\mathbf{r})=N/V=3/(4\pi r_s^3)$, is uniform and so the screening field contribution to the total (N-electron) exchange-correlation energy is given by

$$\begin{aligned}\triangle U_{\mathrm{xc}}&\simeq-\frac{Ne^2}{2}\int d^3r\frac{1}{r_s^3}f(r/r_s)\left(-\frac{2\pi r^2}{3V}\right)\\&=-\frac{e^2}{4r_s}\int d^3(r/r_s)f(r/r_s)[-(r/r_s)^2]. \quad (65)\end{aligned}$$

The exchange-correlation energy per electron therefore contains an extra contribution proportional to $1/(Nr_s)$. The extra contribution is negative since n_{xc} is negative, and hence the quantum Monte Carlo results will contain a negative finite-size error (the energy for small system sizes will come out too low), which is not removed by applying the LDF corrections and which decays like $1/N$. All this is exactly as observed in Fig. 3. Coulomb finite-size corrections of this $1/(Nr_s)$ form have been used before,[6–8,3] but the fact that the corrections should be positive has not been understood before.

The existence of the $1/(Nr_s)$ finite-size effect may also be derived in a more mathematical and perhaps more convincing fashion, which does not rest on physical arguments about finite clusters and metallic screening charges. In the limit when the cubic simulation cell lattice parameter, L, is large, but r is small, we show in Appendix B that

$$\psi(\mathbf{r})-\xi\simeq\frac{1}{r}+\frac{2\pi r^2}{3V}+O(r^4), \quad (66)$$

and the same unwanted quadratic contribution appears.

The simple fact that the Ewald interaction differs from the Coulomb interaction should come as no surprise: the Ewald interaction is periodic and so must depart from the non-periodic $1/r$ form as the simulation cell boundary is approached. What we have done is to determine the leading

contribution to this departure and explain how it gives rise to the long-ranged finite-size errors in the exchange-correlation energy.

Although our explanations have been cast in terms of QMC calculations, it is worth noting that our results are of wider relevance. As pointed out in the recent work of Makov and Payne[1] (which provides an alternative view of some of the questions tackled here), the quadratic terms in the Ewald energy are also responsible for the leading finite-size errors in density-functional calculations for supercells with dipole moments. In addition, we believe that classical simulations of Coulomb liquids should show $1/N$ finite-size errors due to correlations in the ionic positions, and that the same approach we use for QMC calculations (see below) may allow these errors to be reduced. There are also large finite-size errors in Hartree-Fock calculations, which have traditionally been explained in terms of the slow convergence of Brillouin-zone integrals for the exchange energy.[30] As explained in Sec. I, however, using a discrete k-point sampling grid is equivalent to working with a finite simulation cell subject to periodic boundary conditions. Improvements in k-point sampling correspond to increases in the size of the simulation cell, and so this work provides an alternative real-space explanation of the convergence problem. Almost everything we have said about finite-size effects in QMC calculations applies equally well to HF calculations as long as the exchange-correlation hole is replaced by the exchange hole in Eq. (61).

VI. FASTER QUANTUM MONTE CARLO CALCULATIONS WITH SMALLER FINITE-SIZE ERRORS

The last section explained that the $1/(Nr_s)$ finite-size errors are due to the metallic screening charge contribution to the Ewald potential. It also explained that this screening contribution is not present in the cluster definition of the Coulomb energy, and so the finite-size errors would presumably be smaller if we defined our simulation cell Hamiltonian using U_{cluster} instead of U_{Ewald}. Unfortunately, U_{cluster} is not a periodic function of the electronic positions (it differs from the periodic Ewald energy by an electric field term) and so is incompatible with the use of trial functions satisfying periodic boundary conditions. If we want to use U_{cluster} in place of U_{Ewald} then we will also have to abandon the convenient trick of wrapping the system round into a torus.

But all is not lost. We know that in jellium the total energy depends only on the behavior of the effective interaction, $\psi(\mathbf{r}'-\mathbf{r})-\xi$, when $|\mathbf{r}'-\mathbf{r}|$ is small. The Ewald interaction is suitably periodic but contains an unwanted $2\pi|\mathbf{r}'-\mathbf{r}|^2/(3V)$ contribution at small $|\mathbf{r}'-\mathbf{r}|$. All we have to do is modify the Ewald interaction to remove this contribution while making sure that the interaction remains periodic.

We have investigated two different ways of doing this. The first is simply to subtract the appropriate quadratic terms from the Ewald interactions. This method was used by de Leeuw Perram, and Smith[16] in a classical simulation of a hard-sphere dipole fluid, but this is the first time anything similar has been attempted in a QMC calculation. Given charges at $\mathbf{r}'$ and $\mathbf{r}$, we evaluate $\mathbf{r}'-\mathbf{r}$ and reduce it back into the simulation cell centered on the origin by adding a lattice vector if necessary. The resulting reduced difference vector, $\Delta\mathbf{r}$, is then used to work out the quadratic term, $2\pi|\Delta\mathbf{r}|^2/(3V)-C$, which is subtracted from the Ewald interaction to give a new effective interaction. The Ewald interaction is defined so that it averages to zero over the simulation cell, and the presence of the constant,

$$C=\frac{2\pi}{3V^2}\int_{\text{cell}} r^2 d^3r, \tag{67}$$

ensures that the new effective interaction also averages to zero. This is convenient because it guarantees that terms involving the uniform background do not have to be considered explicitly. [Note that C must also be subtracted from the self-energy, ξ, which was defined in Eq. (19) via a limiting process involving the interaction; the value of C therefore cancels out of the expression for the total energy, Eq. (42), as expected.] The reduction of the difference vector into the simulation cell ensures that the effective interaction is periodic as required, but also introduces slope discontinuities when $\Delta\mathbf{r}$ suddenly jumps from one side of the simulation cell to the other. The fact that very good results are obtained despite these discontinuities serves as a convincing confirmation of the theory presented above.

Our second method for reducing the finite-size errors is even more drastic: the difference vector is calculated and reduced into the simulation cell as before, but then we use the simple Coulomb energy, $1/|\Delta\mathbf{r}|-D$, instead of the Ewald interaction. The constant,

$$D=\frac{1}{V}\int_{\text{cell}}\frac{1}{r}d^3r, \tag{68}$$

is again chosen to make sure that the average value of the interaction is zero, and again must be subtracted from the self-energy (which would otherwise be zero in this case). The resulting potential energy is much easier to calculate than the Ewald energy and gives smaller finite-size effects, but again has discontinuities when the reduced difference vector jumps from one side of the simulation cell to the other. Note that the idea of reducing the difference vector into the simulation cell centered on the origin is widely used in classical simulations with short-ranged potentials, where it is known as the minimum image convention;[22] the surprise is that we are using the minimum image convention with the very long-ranged Coulomb interaction.

The changes in simulation cell Hamiltonian affect both the QMC and HF results. It is therefore important to ensure that the same Hamiltonian is used in both sets of calculations when HF energies are used to correct the finite-size errors in QMC results. Our LDF calculations always use the Perdew-Zunger[26] form of the LDA, and so the LDF simulation cell Hamiltonian is the same no matter which many-electron Hamiltonian we are using.

HF and QMC calculations for jellium simulation cells of various sizes were carried out using both the r^2 corrected Ewald interaction and the $1/r$ Hamiltonian. It is clear from Fig. 8 that both Hamiltonians give identical results (to within the statistical errors), as would be expected from our analysis. The residual finite-size errors are much smaller than for the Ewald Hamiltonian, and the slowly decaying $1/N$ com-

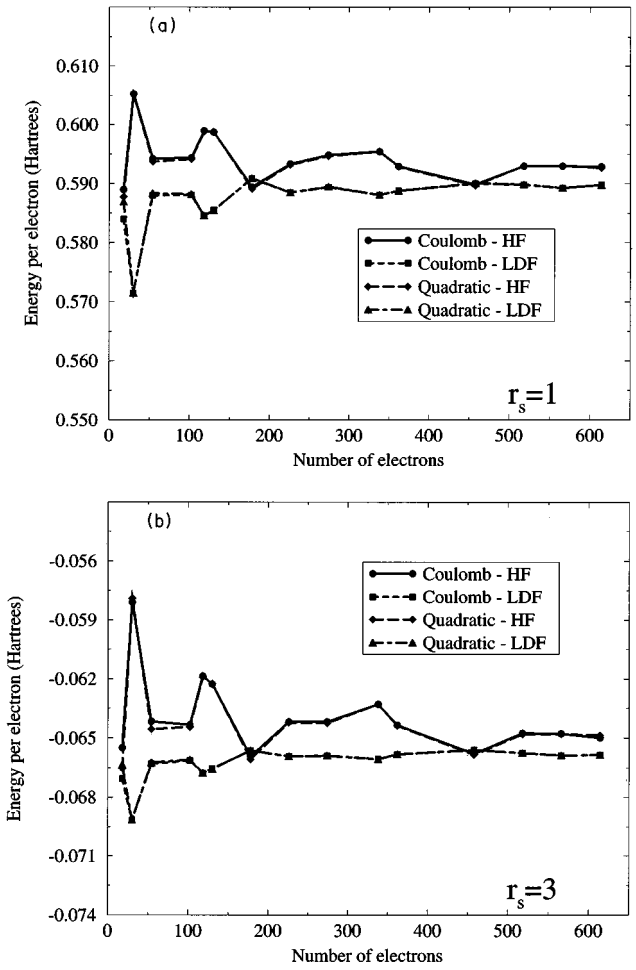

FIG. 8. VQMC results obtained using the new types of model electron-electron interaction. Both the truncated Coulomb interaction and the Ewald interaction with an extra quadratic term have been used, but the results calculated using the two different Hamiltonians are almost indistinguishable. The VQMC results have been corrected using either LDF corrections (the lower pair of lines on each graph) or HF corrections (the upper pair) obtained using the appropriate Hamiltonian. Results are for the densities (a) $r_s=1$ and (b) $r_s=3$.

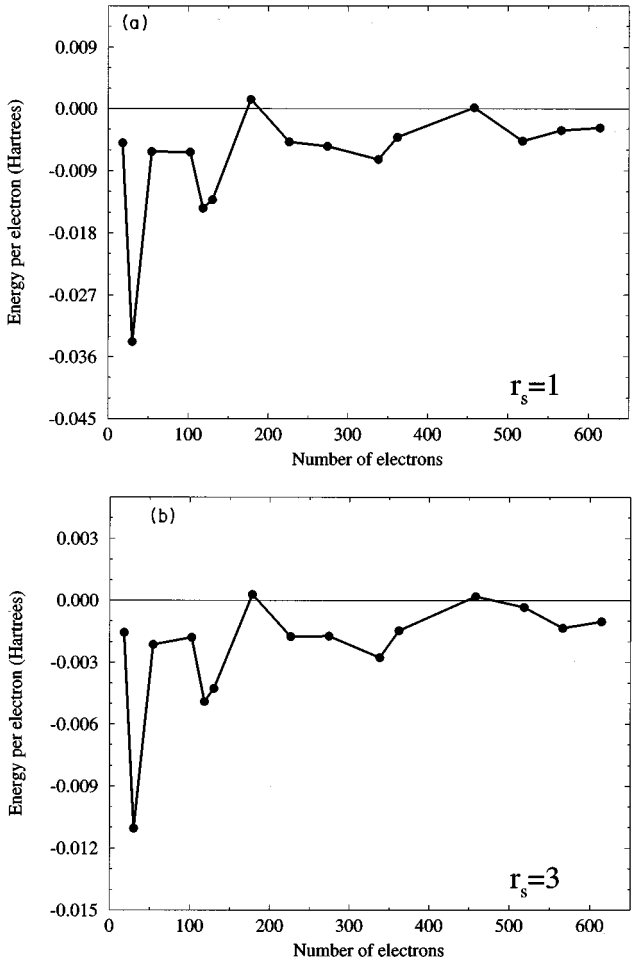

FIG. 9. The difference, ΔV_x, between the LDF finite-size corrections and the HF finite-size corrections for the simulation cell Hamiltonian with truncated Coulomb interactions.

ponent is absent as predicted. The small remaining finite-size errors are presumably due to correlation effects. Since our trial wave functions include correlations by means of the Jastrow factor, that is where one should look if one wants to understand them better.

The difference between the LDF finite-size corrections (ΔT_{1e} only) and the HF finite-size corrections ($\Delta T_{1e}+\Delta V_x$) for these Hamiltonians is also much smaller than for the standard Ewald Hamiltonian. The small difference (ΔV_x) that remains is shown in Fig. 9.

VII. CONCLUSIONS

The finite-size errors present in VQMC calculations for homogeneous systems have been examined carefully and compared to those in other methods. A better understanding of the physical origins of the main finite-size effects has been reached and the question of the optimal definition of the Hamiltonian for simulations using periodic boundary conditions has been clarified. The best choice of $\hat{\mathbf{H}}$ significantly reduces the finite-size errors, which remain after HF or LDF corrections have been applied to VQMC results.

The new Hamiltonian, which contains simple Coulomb interactions treated using the minimum image convention, proves, surprisingly, a much better way to calculate the potential energy than the standard Ewald approach. Ewald summations with quadratic corrections give equally good results, but the evaluation of Ewald sums is computationally costly.

Most of the computer time in conventional jellium QMC calculations is spent doing Ewald summations. This paper has shown that the potential energy is better evaluated using truncated Coulomb interactions, but most QMC programs also use Ewald sums to deal with the slowly decaying $1/r$ tail of the Jastrow factor.[17] There is no doubt that the Jastrow factor should decay like $1/r$ in a metal,[21] but the variational principle guarantees that changing the trial wave function has only a second-order effect on the energy, and so altering the Jastrow factor to make it less costly to evaluate should not change the energy very much.

One approach, introduced by Ortiz and Ballone,[14] is to replace the long-ranged Jastrow factor of Eq. (7) by a different function, which is truncated smoothly at the boundary of the simulation cell with a form determined using Umrigar's

variance minimization technique.[31] For reasonably large simulation cells we have confirmed[32] that this approach gives accurate variational energies comparable to those obtained using standard Jastrow factors. When the use of a short-ranged Jastrow factor is combined with the truncated $1/r$ Hamiltonian introduced in this paper, the result is a HEG QMC code which has no Ewald summations, which runs at least 20 times faster than a conventional program, and which gives results with much smaller finite-size errors.

So far, we have carefully avoided any discussion of finite-size effects in real, inhomogeneous, solids. Ceperley and Alder[7] observed residual finite-size errors of the $1/N$ form in their calculations for solid hydrogen, and we have seen similar $1/N$ errors in our work on Ge.[3] The physical origin of these errors is almost certainly the same as in jellium, and so we ought to be able to improve the QMC results for real solids by altering the simulation cell Hamiltonian just as we did for jellium. Much of the computer time in QMC calculations for real solids is spent evaluating the one-electron wave functions making up the Slater determinant, and so getting rid of the Ewald sums may not improve the performance dramatically; but typical simulation cells for real solids are even smaller than for jellium and so decreasing the finite-size errors is even more important.

Unfortunately, getting rid of the $1/N$ finite-size errors in real solids is more difficult than in jellium since the use of truncated $1/r$ interactions affects the Hartree energy (which is always zero in a homogeneous system) and produces large errors. We are currently investigating one possible solution to this problem and have obtained some encouraging preliminary results, but the work is not yet complete and will be published in a future paper.

Finally, we would like to reemphasize that our analysis of the finite-size errors in QMC calculations can be applied to Coulomb systems in general. Makov and Payne[1] have already pointed out that the quadratic contributions to the Ewald interaction affect supercell LDF calculations. We have now shown that these same quadratic terms produce the $1/N$ finite-size errors in the exchange and exchange-correlation energies of many-electron systems. We have also demonstrated that the $1/N$ errors may be avoided by altering the simulation cell Hamiltonian, and it is possible that similar tricks may prove useful in Hartree-Fock calculations, GW and other many-body calculations, and classical simulations.

ACKNOWLEDGMENTS

We thank David Vanderbilt, Stephen Fahy, and Guy Makov for helpful conversations. Financial support was provided by the Engineering and Physical Sciences Research Council of Great Britain (Grants No. GR/K21061 and No. GR/K42318), and by the European Community via the Human Capital and Mobility Research Network on Quantum Monte Carlo Calculations for Solids (Contract No. CHRX CT94-0462). Most of the computations were carried out on the Cray YMP-8 at the Rutherford-Appleton Laboratory, the Fujitsu VPX240 at Manchester Computing Centre, and the Cray T3D at the Edinburgh Parallel Computing Centre. Some of the development work was carried out on the Cray C-90 at the Pittsburgh Supercomputing Center (Grant No. DMR930039P).

APPENDIX A: QUADRATIC TERMS IN EWALD SUMMATIONS

When studying simple cubic simulation cells containing charges q_i $(i=1,N)$, de Leeuw, Perram, and Smith[16] used the potential energy

$$U=\frac{1}{2}\sum_{i=1}^{N}\sum_{\substack{j=1\\ j\neq i}}^{N} q_i q_j \psi(\mathbf{r}_i-\mathbf{r}_j)+\frac{\xi}{2}\sum_{i=1}^{N} q_i^2+\frac{2\pi}{3V}\left|\sum_{i=1}^{N} q_i \mathbf{r}_i\right|^2, \tag{A1}$$

where the notation is as in Sec. II B. [Note that our notation differs in several respects from theirs: they put $\mathbf{R}=\mathbf{n}L$ and $\mathbf{G}=\mathbf{n}/L$ since they are only considering simple cubic simulation cells, and their definitions of $\psi(\mathbf{r})$ and ξ differ from ours by an additive constant, $\pi/(\kappa^2 V)$.]

Equation (A1) was derived by an explicit summation of $1/r$ Coulomb interactions in an infinite simple cubic lattice. The Coulomb energy of such a system can only be defined if the simulation cell is charge neutral, but even then the sum of $1/r$ interactions is conditionally convergent. De Leeuw, Perram, and Smith[16] concentrated on the value of this sum when one particular order of summation was chosen: to evaluate the Coulomb energy of the cell at the origin, they started by working out the contributions from interactions within that cell itself (U_0); then they added the sum of all the contributions from charges in the first shell of neighboring cells (U_1); then the contributions from the second neighbors (U_2); and so on. At each stage, they included all the charges in a group of cells the centers of which were a given distance from the origin, and these ''spherical shell'' contributions were added together in ascending order of radius. The potential energy at each stage is therefore the energy of the central cell in a large spherical cluster of simulation cells, exactly as defined in Sec. IV B. They were able to show that this spherical shell sum converges (albeit conditionally), and that the same answer may be obtained by taking the limit as $s\rightarrow 0$ of the absolutely convergent sum,

$$\mathbf{U}=\sum_{\text{shells}\ i=1}^{\infty} U_i e^{-s|\mathbf{R}_i|^2}, \tag{A2}$$

where $|\mathbf{R}_i|$ is the length of the lattice vector defining the cells in the ith shell.

For a homogeneous system, the positive background could be thought of as a set of infinitely many, infinitesimally small point charges, and so intuitively the potential energy of Eq. (A1) should be applicable to homogeneous systems as well as to the ionic systems discussed in Ref. 16. That this potential energy can indeed be used for homogeneous systems will be demonstrated below, and the result will be generalized to any lattice. The resulting potential energy is

$$U=\frac{1}{2}\sum_{i=1}^{N}\sum_{\substack{j=1\\ j\neq i}}^{N} e^2\psi(\mathbf{r}_{ij})+\frac{Ne^2\xi}{2}+\frac{2\pi}{3V}\left|\sum_{i=1}^{N} e\mathbf{r}_i\right|^2, \tag{A3}$$

which is simply the ordinary Ewald potential energy for the HEG plus an extra quadratic term.

We will derive this result in two steps. First we sketch out how the de Leeuw, Perram, and Smith derivation[16] for ionic systems may be generalized to an arbitrary Bravais lattice, and then we discuss the limit as the positive ions are smeared out into a uniform jellium background.

We start with the absolutely convergent lattice sum,

$$U(s)=\frac{1}{2}\sum_{i=1}^{N}\sum_{j=1}^{N} q_i q_j \sum_{\mathbf{R}}{}' \frac{e^{-s|\mathbf{R}|^2}}{|\mathbf{r}_{ij}+\mathbf{R}|}, \tag{A4}$$

where the prime on the $\mathbf{R}$ summation means that the $\mathbf{R}=\mathbf{0}$ term is to be omitted when $i=j$. If we now define

$$\tilde{\psi}(\mathbf{r},s)=\sum_{\mathbf{R}} \frac{e^{-s|\mathbf{R}|^2}}{|\mathbf{r}+\mathbf{R}|}, \tag{A5}$$

the expression for $U(s)$ may be rewritten in the form

$$U(s)=\frac{1}{2}\sum_{i=1}^{N}\sum_{\substack{j=1\\ j\neq i}}^{N} q_i q_j \tilde{\psi}(\mathbf{r}_{ij},s) + \frac{1}{2}\sum_{i=1}^{N} q_i^2 \lim_{|\mathbf{r}|\to 0}\left(\tilde{\psi}(\mathbf{r},s)-\frac{1}{|\mathbf{r}|}\right). \tag{A6}$$

To evaluate $U(s)$ a new representation of $\tilde{\psi}(\mathbf{r},s)$ is needed. The identities that are used are

$$x^{-1}=\frac{1}{\sqrt{\pi}}\int_0^\infty t^{-1/2}e^{-tx^2}dt \tag{A7}$$

and the Fourier series,

$$\sum_{\mathbf{R}} e^{-t(\mathbf{r}+\mathbf{R})^2}=\frac{1}{V}\left(\frac{\pi}{t}\right)^{3/2}\sum_{\mathbf{G}} e^{2\pi i\mathbf{G}\cdot\mathbf{r}-\pi^2G^2/t}. \tag{A8}$$

Using the first identity, the $|\mathbf{r}+\mathbf{R}|^{-1}$ factor in Eq. (A5) is replaced by an integral, which is then split into two integrals at an arbitrary point $t=\kappa^2$ giving

$$\tilde{\psi}(\mathbf{r},s)=\sum_{\mathbf{R}}\frac{1}{\sqrt{\pi}}\int_{\kappa^2}^\infty dt\, t^{-1/2}\exp[-s|\mathbf{R}|^2-t|\mathbf{r}+\mathbf{R}|^2] + \sum_{\mathbf{R}}\frac{1}{\sqrt{\pi}}\int_0^{\kappa^2} dt\, t^{-1/2} \times\exp\left[-\frac{st|\mathbf{r}^2|}{s+t}-(s+t)\left|\mathbf{R}+\frac{t\mathbf{r}}{s+t}\right|^2\right]. \tag{A9}$$

Using the second identity this becomes

$$\tilde{\psi}(\mathbf{r},s)=\sum_{\mathbf{R}}\frac{1}{\sqrt{\pi}}\int_{\kappa^2}^\infty dt\, t^{-1/2}\exp[-s|\mathbf{R}|^2-t|\mathbf{r}+\mathbf{R}|^2] + \frac{\pi}{V}\sum_{\mathbf{G}}\int_0^{\kappa^2} dt\,\frac{1}{t^{1/2}(s+t)^{3/2}} \times\exp\left[\frac{-st|\mathbf{r}|^2-\pi^2|\mathbf{G}|^2+2\pi it\mathbf{G}\cdot\mathbf{r}}{s+t}\right]. \tag{A10}$$

Both these integrals may be evaluated analytically (see de Leeuw, Perram, and Smith[16] for the mathematical details) to give

$$\begin{aligned}\tilde{\psi}(\mathbf{r},s)&=\frac{1}{V}\sum_{\mathbf{G}\neq 0}\frac{\exp[-\pi^2G^2/\kappa^2+2\pi i\mathbf{G}\cdot\mathbf{r}]}{\pi G^2} - \frac{\pi}{V\kappa^2}+\sum_{\mathbf{R}}\frac{\operatorname{erfc}(\kappa|\mathbf{R}+\mathbf{r}|)}{|\mathbf{R}+\mathbf{r}|} + \frac{2\pi}{Vs}-\frac{2\pi}{3V}|\mathbf{r}|^2+O(s)\\ &=\psi(\mathbf{r})+\frac{2\pi}{Vs}-\frac{2\pi}{3V}|\mathbf{r}|^2+O(s),\end{aligned} \tag{A11}$$

where $\psi(\mathbf{r})$ is as defined in Sec. II B. Substituting back into Eq. (A6) and remembering the definition of ξ,

$$\xi=\lim_{\mathbf{r}\to\mathbf{0}}\left(\psi(\mathbf{r})-\frac{1}{|\mathbf{r}|}\right), \tag{A12}$$

gives

$$U(s)=\frac{1}{2}\sum_{i=1}^{N}\sum_{\substack{j=1\\ j\neq i}}^{N} q_i q_j\left(\psi(\mathbf{r}_{ij})-\frac{2\pi}{3V}|\mathbf{r}_{ij}|^2\right) + \frac{1}{2}\sum_{i=1}^{N}\sum_{j=1}^{N} q_i q_j\frac{2\pi}{Vs}+\frac{1}{2}\sum_{i=1}^{N} q_i^2\xi+O(s). \tag{A13}$$

The $1/s$ term vanishes because of charge neutrality and so the limit as $s\to 0$ is easily taken. Charge neutrality also implies that

$$\sum_{i=1}^{N}\sum_{j=1}^{N} q_i q_j|\mathbf{r}_i-\mathbf{r}_j|^2=-2\sum_{i=1}^{N}\sum_{j=1}^{N} q_i q_j\mathbf{r}_i\cdot\mathbf{r}_j \tag{A14}$$

and hence Eq. (A1) is obtained.

The corresponding results for a jellium cell may now be found by considering the limit in which the simulation cell contains N unit negative charges (the electrons) and a very large number of very small uniformly distributed positive charges which sum up to ensure charge neutrality. As the number of positive charges becomes larger and the charge of each becomes correspondingly smaller, the self-interaction (ξ) contribution from the distribution of positive charges becomes negligible. Furthermore, since the average value of $\psi(\mathbf{r})$ within the simulation cell is zero, all ψ terms involving the positive charges may be neglected and Eq. (A1) reduces to

$$U=\frac{1}{2}\sum_{i=1}^{N}\sum_{\substack{j=1\\ j\neq i}}^{N} e^2\psi(\mathbf{r}_{ij})+\frac{Ne^2\xi}{2}+\frac{2\pi}{3V}|\mathbf{p}|^2, \quad \text{(A15)}$$

where $\mathbf{p}$ is the total dipole moment of the simulation cell. This in turn reduces to Eq. (A3) as long as the origin of coordinates is chosen so that the dipole moment of the positive background charge is zero.

APPENDIX B: SHORT-RANGE BEHAVIOR OF THE EWALD INTERACTION IN LARGE SIMULATION CELLS OF CUBIC SYMMETRY

The expression for the exchange-correlation energy, Eq. (61), involves the "Ewald interaction" $\psi(\mathbf{r})-\xi$. Using the definitions of $\psi(\mathbf{r})$ and ξ from Eqs. (16) and (19), this may be written in the form

$$\psi(\mathbf{r})-\xi=\sum_{\mathbf{R}}\frac{\mathrm{erfc}(\kappa|\mathbf{r}-\mathbf{R}|)}{|\mathbf{r}-\mathbf{R}|}-\sum_{\mathbf{R}(\neq\mathbf{0})}\frac{\mathrm{erfc}(\kappa R)}{R}+\frac{1}{V}\sum_{\mathbf{G}(\neq\mathbf{0})}\frac{\exp(-\pi^2G^2/\kappa^2+2\pi i\mathbf{G}\cdot\mathbf{r})}{\pi G^2}-\frac{1}{V}\sum_{\mathbf{G}(\neq\mathbf{0})}\frac{\exp(-\pi^2G^2/\kappa^2)}{\pi G^2}+\frac{2\kappa}{\sqrt{\pi}}. \quad \text{(B1)}$$

We wish to determine the contributions that give rise to the exchange-correlation finite-size errors in cubic systems; these are terms that are important at small r and decay only slowly as the simulation cell size increases.

We start by considering the two real space sums. The terms with $\mathbf{R}\neq\mathbf{0}$ decrease at least as fast as $\exp(-\kappa^2L^2)$, where L is the length of the shortest simulation cell lattice vector, and so rapidly become negligible as the simulation cell size increases. Expanding the $\mathbf{R}=\mathbf{0}$ term as a power series in r then gives

$$\mathbf{R}\text{ space sums}=\frac{1}{r}-\frac{2\kappa}{\sqrt{\pi}}+\frac{2\kappa^3r^2}{3\sqrt{\pi}}+O(r^4). \quad \text{(B2)}$$

The two reciprocal space sums are a little harder to deal with. The $e^{2\pi i\mathbf{G}\cdot\mathbf{r}}$ factors in the first sum can be expanded as power series in $\mathbf{r}$, and the $\mathbf{r}$-independent terms then cancel the second sum. The odd powers of $\mathbf{r}$ contribute nothing because of the inversion symmetry of the simulation cell reciprocal lattice and hence,

$$\mathbf{G}\text{ space sums}=\frac{1}{V}\sum_{\mathbf{G}\neq\mathbf{0}}\frac{e^{-\pi^2G^2/\kappa^2}}{\pi G^2}\left(-\frac{4\pi^2(\mathbf{G}\cdot\mathbf{r})^2}{2}\right)+O(r^4). \quad \text{(B3)}$$

Working in Cartesian coordinates, $(\mathbf{G}\cdot\mathbf{r})^2=(G_xx+G_yy+G_zz)^2$, and noting that the cross terms sum to zero because of the cubic symmetry, one obtains

$$\mathbf{G}\text{ space sums}=-\frac{2\pi r^2}{3V}\sum_{\mathbf{G}\neq\mathbf{0}}e^{-\pi^2G^2/\kappa^2}. \quad \text{(B4)}$$

The remaining sum may be evaluated by setting $\mathbf{r}=\mathbf{0}$ in the familiar Fourier series,

$$\sum_{\mathbf{R}}e^{-\kappa^2(\mathbf{r}-\mathbf{R})^2}=\frac{\pi^{3/2}}{\kappa^3V}\sum_{\mathbf{G}}e^{2\pi i\mathbf{G}\cdot\mathbf{r}-\pi^2G^2/\kappa^2}, \quad \text{(B5)}$$

to obtain

$$\mathbf{G}\text{ space sums}=-\frac{2\pi r^2}{3V}\left[\frac{\kappa^3V}{\pi^{3/2}}\sum_{\mathbf{R}}e^{-\kappa^2R^2}-1\right]=\frac{2\pi r^2}{3V}-\frac{2\kappa^3r^2}{3\sqrt{\pi}}+O(e^{-\kappa^2L^2}). \quad \text{(B6)}$$

Finally, combining the results for the real and reciprocal space sums, we find

$$\psi(\mathbf{r})-\xi=\frac{1}{r}+\frac{2\pi r^2}{3V}+O(r^4), \quad \text{(B7)}$$

which shows the slowly decaying quadratic finite-size correction discussed in Sec. V.

[1] G. Makov and M. C. Payne, Phys. Rev. B **51**, 4014 (1995).
[2] G. Rajagopal, R. J. Needs, S. Kenny, W. M. C. Foulkes, and A. J. James, Phys. Rev. Lett. **73**, 1959 (1994).
[3] G. Rajagopal, R. J. Needs, A. James, S. D. Kenny, and W. M. C. Foulkes, Phys. Rev. B **51**, 10 591 (1995).
[4] X.-P. Li, D. M. Ceperley, and R. M. Martin, Phys. Rev. B **44**, 10 929 (1991).
[5] L. Mitáš and R. M. Martin, Phys. Rev. Lett. **72**, 2438 (1994).
[6] D. M. Ceperley and B. J. Alder, Phys. Rev. Lett. **45**, 566 (1980).
[7] D. M. Ceperley and B. J. Alder, Phys. Rev. B **36**, 2092 (1987).
[8] G. Sugiyama, G. Zerah, and B. J. Alder, Physica A **156**, 144 (1989).
[9] M. P. Tosi, in *Solid State Physics: Advances in Research and Applications*, edited by H. Ehrenreich and D. Turnbull (Academic, New York, 1964), Vol. 16, p. 1.
[10] E. L. Pollock and B. J. Alder, Physica A **102**, 1 (1980).
[11] B. J. Alder and E. L. Pollock, Annu. Rev. Phys. Chem. **32**, 311 (1981).
[12] M. Neumann, O. Steinhauser, and G. S. Pawley, Mol. Phys. **52**, 97 (1984).
[13] S. W. de Leeuw, J. W. Perram, and E. R. Smith, Annu. Rev. Phys. Chem. **37**, 245 (1986).
[14] G. Ortiz and P. Ballone, Europhys. Lett. **23**, 7 (1993).
[15] G. Ortiz and P. Ballone, Phys. Rev. B **50**, 1391 (1994).
[16] S. W. de Leeuw, J. W. Perram, and E. R. Smith, Proc. R. Soc. London Ser. A **373**, 27 (1980).
[17] S. Fahy, X. W. Wang, and S. G. Louie, Phys. Rev. B **42**, 3503 (1990).
[18] M. H. Kalos and P. A. Whitlock, *Monte Carlo Methods, Vol. 1: Basics* (Wiley, New York, 1986).
[19] B. L. Hammond, W. A. Lester, and P. J. Reynolds, *Monte Carlo Methods in Ab Initio Quantum Chemistry* (World Scientific, Singapore, 1994).

[20] N. Metropolis, A. W. Rosenbluth, M. N. Rosenbluth, A. H. Teller, and E. Teller, J. Chem. Phys. **21**, 1087 (1953).
[21] D. M. Ceperley, Phys. Rev. B **18**, 3126 (1978).
[22] M. P. Allen and D. J. Tildesley, *Computer Simulation of Liquids* (Clarendon, Oxford, 1987).
[23] G. Rajagopal and R. J. Needs, J. Comput. Phys. **115**, 399 (1994).
[24] J. Callaway and N. H. March, in *Solid State Physics: Advances in Research and Applications*, edited by H. Ehrenreich and D. Turnbull (Academic, New York, 1984), Vol. 38, p. 135.
[25] R. G. Parr and W. Yang, *Density-Functional Theory of Atoms and Molecules* (Oxford University Press, Oxford, 1989).
[26] J. Perdew and A. Zunger, Phys. Rev. B **23**, 5048 (1981).
[27] C. Kittel, *Introduction to Solid State Physics*, 3rd ed. (Wiley, New York, 1966), Chap. 12.
[28] J. D. Jackson, *Classical Electrodynamics*, 2nd ed. (Wiley, New York, 1975), Sec. 5.10.
[29] O. Madelung, *Introduction to Solid State Theory*, 2nd printing, Springer Series in Solid State Sciences Vol. 2 (Springer-Verlag, Berlin, 1978), Sec. 3.1.3.
[30] W. von der Linden and P. Horsch, Phys. Rev. B **37**, 8351 (1988).
[31] C. J. Umrigar, K. G. Wilson, and J. W. Wilkins, Phys. Rev. Lett. **60**, 1719 (1988).
[32] A. J. Williamson, G. Rajagopal, A. J. James, R. J. Needs, S. D. Kenny, and W. M. C. Foulkes (unpublished).